

**STUDY OF THE IMPACT OF NON-DETERMINISM ON  
NUMERICAL REPRODUCIBILITY  
AND DEBUGGING AT THE EXASCALE**

by

Dylan Chapp

A thesis submitted to the Faculty of the University of Delaware in partial fulfillment of the requirements for the degree of Master of Science in Computer Science

Spring 2017

© 2017 Dylan Chapp  
All Rights Reserved

**STUDY OF THE IMPACT OF NON-DETERMINISM ON  
NUMERICAL REPRODUCIBILITY  
AND DEBUGGING AT THE EXASCALE**

by

Dylan Chapp

Approved: \_\_\_\_\_  
Michela Taufer, Ph.D.  
Professor in charge of thesis on behalf of the Advisory Committee

Approved: \_\_\_\_\_  
Kathleen McCoy, Ph.D.  
Chair of the Department of Computer and Information Sciences

Approved: \_\_\_\_\_  
Babatunde A. Ogunnaike, Ph.D.  
Dean of the College of Engineering

Approved: \_\_\_\_\_  
Ann L. Ardis, Ph.D.  
Senior Vice Provost for Graduate and Professional Education

## ACKNOWLEDGMENTS

I want to thank my advisor Dr. Michela Taufer for her tireless commitment to my growth as a researcher, and for shepherding my exploration of the HPC research community. I want to thank my mentors at Lawrence Livermore National Lab, Dr. Kento Sato and Dong H. Ahn, whose impact on my work has been transformative both during my time at LLNL and beyond. I want to thank Dr. Travis Johnston for his mentorship during my first year of graduate studies. I want to thank Dr. Sunita Chandrasekaran for her service on my committee and her advice during the final stages of my work. I also extend my sincere appreciation to all of the members of GCLab, past and present, for their advice and company.

Finally I want to thank my parents, Jeff and Belena, whose love and support has extracted me from countless local minima, and Alicia, who impressed upon me the value of lists.

# TABLE OF CONTENTS

<b>LIST OF TABLES</b> . . . . .	<b>vi</b>
<b>LIST OF FIGURES</b> . . . . .	<b>vii</b>
<b>ABSTRACT</b> . . . . .	<b>x</b>
 <b>Chapter</b>	
<b>1 INTRODUCTION</b> . . . . .	<b>1</b>
1.1 Problem Overview and Proposed Solutions . . . . .	1
1.1.1 Overview of Numerical Challenge . . . . .	2
1.1.2 Overview of the Debugging Challenge . . . . .	3
1.2 Thesis Statement . . . . .	4
1.3 Contributions . . . . .	4
1.4 Thesis Outline . . . . .	5
<b>2 THE NUMERICAL CHALLENGE</b> . . . . .	<b>6</b>
2.1 Introduction . . . . .	6
2.2 Sources of Numerical Inaccuracy . . . . .	6
2.2.1 Nonassociativity: A Consequence of Finite Precision . . . . .	6
2.2.2 High Concurrency: A Consequence of Extreme Scale . . . . .	7
2.3 Mathematical Techniques . . . . .	9
2.3.1 Fixed-Reduction Order . . . . .	10
2.3.2 Interval Arithmetic . . . . .	10
2.3.3 High-Precision Arithmetic . . . . .	11
2.3.4 Compensated Summation Algorithms . . . . .	11

2.3.5	Prerounded Summation Algorithms . . . . .	12
2.4	Inadequacy of Conventional Wisdom . . . . .	12
2.4.1	Using Analytical Error Bounds . . . . .	12
2.4.2	Tracking Cancellations . . . . .	13
2.4.3	Choice of Summation Algorithm . . . . .	15
2.5	Exploring the Reproducibility Space . . . . .	18
2.5.1	Experimental Environment and Parameters . . . . .	19
2.5.2	Sensitivity of Summation Algorithms . . . . .	21
2.5.3	Effect of Concurrency, Conditioning, and Dynamic Range . . .	24
2.5.4	Intelligent Selection of Reduction Algorithms . . . . .	27
2.6	Lessons Learned . . . . .	28
<b>3</b>	<b>THE DEBUGGING CHALLENGE . . . . .</b>	<b>30</b>
3.1	Introduction . . . . .	30
3.2	Record-and-Replay Approach and Tools . . . . .	30
3.3	Clock-Delta Compression . . . . .	32
3.4	Logical Clocks . . . . .	33
3.5	In- and Out-of-order Received Messages . . . . .	34
3.6	Permutation Encoding . . . . .	36
3.7	Logical Clock Ticking Policies . . . . .	39
3.8	Applicability to Real Applications with Real Record-and-Replay Tool	41
3.9	Assessing Different Ticking Policies . . . . .	42
3.9.1	Experimental Setting . . . . .	42
3.9.2	Results . . . . .	44
3.10	Lessons Learned . . . . .	46
<b>4</b>	<b>CONCLUSION AND FUTURE WORK . . . . .</b>	<b>49</b>
4.1	Introduction . . . . .	49
4.2	Out-of-Order Events and Communication Patterns . . . . .	49
4.3	Adaptive Ticking Policies . . . . .	55
4.4	Investigating Numerical Irreproducibility via Record-and-replay . . .	55
4.5	Summary . . . . .	56
	<b>BIBLIOGRAPHY . . . . .</b>	<b>57</b>

## LIST OF TABLES

1.1	Concurrency trends in high performance computing platforms. (Expected increase in concurrency in bold) . . . . .	1
2.1	Example of sample set of values with specified dynamic range, $dr$ , and condition number, $k$ . . . . .	21

## LIST OF FIGURES

1.1	Two examples of non-determinism associated to message passing executions. . . . .	4
2.1	Two reduction trees at the opposite ends of the spectrum. . . . .	8
2.2	Empirical study of error magnitudes and worst-case error bounds for 10,000 summations of 10,000 values randomly sorted. . . . .	14
2.3	Empirical study of cancellations vs. error magnitude for different summation orders. . . . .	16
2.4	Comparison of execution time to sum $10^6$ terms for standard summation (ST), Kahan's compensated summation (K), composite precision summation (CP), and prerounded summation (PR). . . . .	17
2.5	Performance losses of Kahan's compensated summation (K), composite precision (CP), and prerounded (PR) summations compared to the standard summation (ST). . . . .	18
2.6	Empirical study of relative sensitivity of three summation algorithms: Kahan's compensated summation (K), composite precision summation (CP), and prerounded summation (PR). Note that (a) zooms into (b). . . . .	19
2.7	Error distributions for the four summation algorithms considered in this chapter for balanced and unbalanced reductions: three at a smaller (8K leaves) and one at higher (1M leaves) levels of concurrency. . . . .	23
2.8	Overview of the grid with its cells used to study the effect of concurrency, conditioning, and dynamic range. . . . .	25
2.9	Standard deviation errors for standard summation (left), Kahan summation (middle), and composite precision summation (right) for different $(k, dr)$ values and fixed concurrency $n$ . . . . .	25

2.10	Standard deviation errors for standard summation (left), Kahan summation (middle), and composite precision summation (right) for different $(n, dr)$ values and fixed condition number $k$ . . . . .	26
2.11	Standard deviation errors for standard summation (left), Kahan summation (middle), and composite precision summation (right) for different $(n, k)$ values and fixed dynamic range $dr$ . . . . .	26
2.12	Selection of the cheapest but acceptably accurate reduction algorithm among the Kahan (K), composite precision (CP), and prrounding (PR) algorithms for different error variability thresholds (left to right: $t = 5e - 13, 3e - 13, 2.5e - 13, 1.5e - 13, 5e - 14$ ). . . . .	28
3.1	General overview of a record-and-replay framework. . . . .	31
3.2	Example of in-order (a) and out-of-order (b) messages. . . . .	35
3.3	Example of a five-stage execution in which in-order and out-of-order messages are received by process $P_0$ . We show in-order receives in stages 1, 2, 3, and 5. We show an out-of-order receive in stage 4, in which a sent clock of 4 is received after $P_0$ has already received a larger sent clock of 5. . . . .	37
3.4	Process to transform a totally in-order set of message receives into the order we observed for Figure 3.3. . . . .	38
3.5	Steps performed by the replay stage in a record-and-replay tool to recreate the observed execution built during the record stage. . . .	39
3.6	High level overview of the three ticking policies considered in this work: (a) basic ticking, (b) wall-clock ticking, and (c) FLOPs-based ticking. . . . .	40
3.7	MCB communication patterns: the neighbor-to-neighbor particle exchange (a), the non-blocking gather (b), and the non-blocking scatter (c). . . . .	41
3.8	Tested scenarios (in green cells) in the space of application parameters considered in this thesis. Gray cells are left for future work. . . . .	43



3.9	Distributions of out-of-order message percentages and median out-of-order percentage for each ticking policy over all executions on a <b>single node</b> of Vulcan. The test cases are: 1K particles per process, buffer size 5 (a); 1K particles per process, buffer size 5K (b); 1M particles per process, buffer size 5 (c); and 1M particles per process, buffer size 5K (d). . . . .	44
3.10	Distributions of out-of-order message percentages and median out-of-order percentage for each ticking policy over all executions on <b>four nodes</b> of Vulcan. The test cases are: 1K particles per process, buffer size 5 (a); 1K particles per process, buffer size 5K (b); 1M particles per process, buffer size 5 (c); and 1M particles per process, buffer size 5K (d). . . . .	46
3.11	Distributions of out-of-order message percentages and median out-of-order percentage for each ticking policy over all executions on <b>16 nodes</b> of Vulcan. The test cases are: 1K particles per process, buffer size 5 (a); 1K particles per process, buffer size 5K (b); 1M particles per process, buffer size 5 (c); and 1M particles per process, buffer size 5K (d). . . . .	47
4.1	Interpreting a heatmap of message receives. The receiving processes are listed per row; the sending processes are listed per column. . . .	51
4.2	Total number of messages received by each receiving process $i$ per sender process $j$ for a testcase of 1K particles per process, buffer size 5 (a); 1K particles per process, buffer size 5K (b); 1M particles per process, buffer size 5 (c); and 1M particles per process, buffer size 5K (d). . . . .	52
4.3	Total number of out-of-order messages received by each receiving process $i$ per sender process $j$ for a test case of 1K particles per process, buffer size 5 (a); 1K particles per process, buffer size 5K (b); 1M particles per process, buffer size 5 (c); and 1M particles per process, buffer size 5K (d). . . . .	53
4.4	Linking out-of-order receives to one of the three MCB communication patterns presented in Figure 3.7. Because of space constraints only a quarter of each heatmap is shown. Each row shows heatmaps with receiving processes highlighted that participate in a given communication pattern. Column (a) shows heatmaps of total number of receives; column (b) shows the communication pattern; and column (c) shows heatmaps of the number of out-of-order receives. . . . .	54

## ABSTRACT

Non-determinism in high performance scientific applications has severe detrimental impacts for both numerical reproducibility and accuracy, and debugging. As scientific simulations are migrated to extreme-scale platforms, the increase in platform concurrency and the attendant increase in non-determinism is likely to exacerbate both of these problems. In this thesis, we address the dual challenges of non-determinism’s impact on numerical reproducibility and on debugging.

To address the numerical challenge, our work investigates the power of mathematical methods to mitigate error propagation at the exascale. We focus on floating-point error accumulation over global summations where enforcing any reduction order is expensive or impossible. We model parallel summations with reduction trees and identify those parameters that can be used to estimate the reduction’s sensitivity to variability in the reduction tree. We assess the impact of these parameters on the ability of different reduction methods to successfully mitigate errors. Our results illustrate the pressing need for intelligent runtime selection of reduction operators that ensure a given degree of reproducible accuracy.

To address the debugging challenge, our work examines the impact of logical clock ticking policies on the Clock-Delta Compression record-and-replay technique. We assess three logical clock ticking policies in terms of the number of out-of-order messages that result during recording executions under these policies. We examine the performance of Clock-Delta Compression when using the three ticking policies in four distinct application scenarios to probe the impact of floating-point workload and communication intensity on recording performance. Our results illustrate the pressing need for fine-grained logical clock ticking policies that reduce the out-of-order message rate of the Clock-Delta Compression record-and-replay technique.

## Chapter 1

### INTRODUCTION

#### 1.1 Problem Overview and Proposed Solutions

Scientific simulations are increasingly being migrated to extreme-scale platforms consisting of hundreds (or thousands) of multicore servers equipped with many-core accelerators. The increasing number of nodes and cores is resulting in an increasing level of concurrency and ultimately non-determinism in the execution of large scale applications on these platforms. Table 1.1 shows the concurrency levels in 2010 and the expected levels in 2023.

	<b>2010</b>	<b>2023</b>	<b>Factor Change</b>
System Peak	2 Pf/s	1 Ef/s	500
Power	6 MW	20 MW	3
System Memory	0.3 PB	32 PB	100
Node Performance	0.125 Gf/s	10 Tf/s	80
Node Memory BW	25 GB/s	400 GB/s	16
Node Concurrency	12 cpus	1000 cpus	83
Interconnect BW	1.5 GB/s	200 GB/s	133
System Size (nodes)	20 K nodes	1 M nodes	50
<b>Total Concurrency</b>	<b>225 K</b>	<b>1 B</b>	<b>4,444</b>
Storage	15 PB	300 PB	20
Input/Output BW	0.2 TB/s	20 TB/s	100

**Table 1.1:** Concurrency trends in high performance computing platforms. (Expected increase in concurrency in bold)

From the perspective of reproducibility of applications, the trade-off between performance and determinism presents two distinct challenges. First, permitting non-deterministic ordering of interprocess communication opens the door to numerical irreproducibility via the interaction between reduction order and the non-associativity

of floating-point arithmetic. This is defined in this thesis as the numerical challenge.

Second, non-determinism significantly hampers debugging efforts during application development and scaling. Specifically, there exist cases where bugs manifest only during some executions due to a particular ordering of message receives. If the application does not guarantee a specific message receive order then this class of bugs becomes very hard to diagnose and treat since the cost of reproducing them significantly increases. Recent work by Sato *et. al* [26], presents a case-study of the impact of a non-deterministic bug in terms of developer time and computational resources. This is defined in this thesis as the debugging challenge.

### 1.1.1 Overview of Numerical Challenge

Because floating-point numbers have finite precision, no simulation can be completely free of error. As hardware resources grow, the scientific computation taking advantage of that hardware has become increasingly complex. A consequence of the scale of computation is that even small errors at the beginning of the simulation may eventually compound into significant accuracy problems, which may call into question the validity of hours and hours of computation. Multithreading complicates matters by introducing nondeterminism. Not only do errors accumulate throughout a computation, but a scientist may run the same computation several times with differing results. According to a recent report from the Department of Energy [2], by the end of this decade the level of concurrency of the supercomputing platforms on which simulations are executed is expected to increase by a factor of at least 4000. The question that must be answered is: Can the scientific community trust simulations executed on next-generation exascale architectures?

In Chapter 2, we assess the effectiveness of several mathematical techniques to pursue reproducible accuracy on exascale platforms with multithreading hardware consisting of multicore processors coupled with many-core accelerators. We refer to *reproducibility* as “closeness of agreement among repeated simulation results under the same initial conditions” and *accuracy* as “conformity of a resulting value to an

accepted standard, or scientific laws” (from Van Nostrands Scientific Encyclopedia). Rather than focusing on bitwise reproducibility, we study methodologies to minimize the propagation of errors and, thereby, limit their impact on the results of a simulation, increasing both the reproducibility of the simulation and the meaningfulness of the results.

### 1.1.2 Overview of the Debugging Challenge

Application developers employ a variety of programming techniques to maximize the scalability of their applications on the increasingly concurrent platforms. In the case of message-passing applications, one notable technique is the use of non-blocking point-to-point communication, which permits communication and computation to be overlapped, leading to an increase in scalability. The price paid however, is the loss of determinism mentioned above. The program’s interprocess communication does not behave exactly the same way during each execution. Figure 1.1 shows two high level examples of non-deterministic executions when the same destinations received the messages in different orders and when messages are exchanged between two different destinations. This problem is further exacerbated by use of wildcard receives (i.e., permitting a process to receive its next message from any available sender, rather than a specific one). This non-determinism impedes debugging efforts by vastly increasing the cost in computational resources and developer time needed to reproduce bugs, necessitating the use of record-and-replay tools. The question we address is: How can record-and-replay tools be improved so that they can continue to enable debugging on future exascale systems.

In Chapter 3, we assess the effectiveness of multiple logical clock ticking policies, including a novel ticking policy we develop, when used as the underlying ordering mechanism in Clock-Delta Compression (CDC), a state-of-the-art record-and-replay technique. We evaluate ticking policies’ effectiveness in enabling CDC’s compression against a real application in a diverse set of runtime conditions that reflect variability in floating-point workload and communication intensity that HPC applications exhibit.

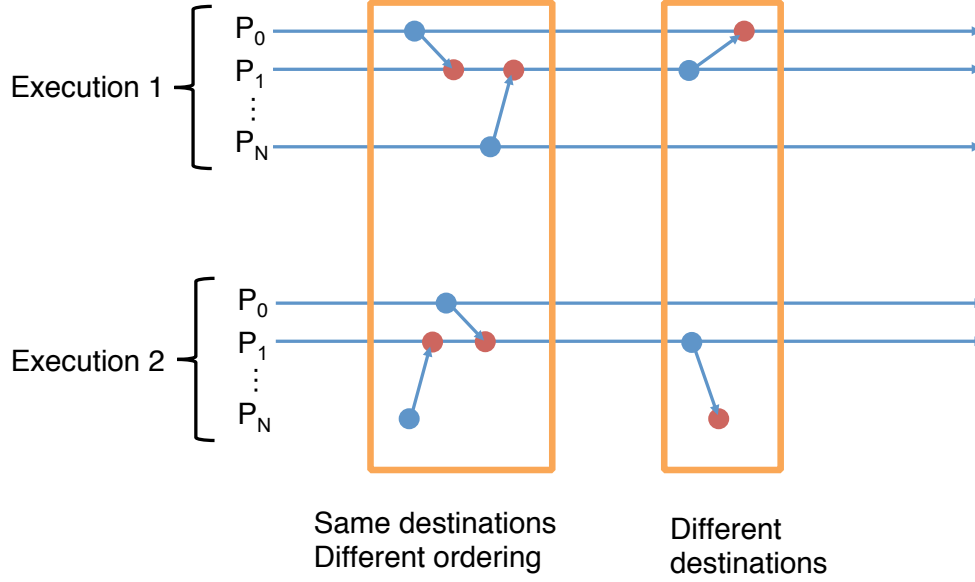


**Figure 1.1:** Two examples of non-determinism associated to message passing executions.

## 1.2 Thesis Statement

We claim that the massive increase in total system concurrency that will accompany exascale systems will significantly amplify the problems of numerical irreproducibility and impeded debugging that HPC developers currently face. We address the numerical challenge of reproducibility by illustrating the pressing need for intelligent runtime selection of reduction operators for problematic floating-point inputs. We address the debugging challenge by demonstrating the pressing need for logical clock ticking policies that reduce then out-of-order message rate of the Clock-Delta Compression record-and-replay technique.

## 1.3 Contributions

When dealing with the numerical challenge, our contributions are as follows:

- We evaluate and compare the reproducibility of four summation techniques applied to a simulated exascale environment.
- We demonstrate that commonly accepted practices for predicting and mitigating errors offer incomplete characterizations of the reproducibility of numerical algorithms when applied in isolation.

- We demonstrate the need for data-aware software to intelligently choose reduction algorithms to guarantee reproducibility without an unnecessary loss in performance.

When dealing with the debugging challenge, our contributions are as follows:

- We propose a logical clock ticking policy based on floating-point operations that can be integrated in Clock-Delta Compression.
- We provide a comparison of three ticking policies’ (basic Lamport clock ticking, wall-time-based ticking, and FLOPs-based ticking) effectiveness under diverse runtime conditions.
- We demonstrate the potential for extending logical clock ticking policies to adapt to applications’ non-deterministic communication patterns.

## 1.4 Thesis Outline

Chapter 2 introduces our work on reproducible numerical accuracy, and presents results on selection of compensated summation algorithms based on mathematical properties of summands. Chapter 3 introduces our work on record-and-replay tools, and presents results on our fine-grained logical clock ticking policy as applied to the Clock-Delta Compression record-and-replay technique. Chapter 4 lays out the plan for extending our research on reproducibility in HPC by applying the lessons learned in Chapter 2 and Chapter 3 to non-deterministic communication patterns extracted from applications.

## Chapter 2

### THE NUMERICAL CHALLENGE

#### 2.1 Introduction

In this chapter we first summarize both well-known and emerging sources of numerical inaccuracy and describe techniques for supporting reproducible accuracy. We then prove the inadequacy of conventional wisdom when dealing with this problem and provide strong evidence of the need for intelligent reduction operations at the extreme scale before to conclude the chapter with a short summary of our learned lessons.

#### 2.2 Sources of Numerical Inaccuracy

Achieving reproducible numerical accuracy at exascale faces two fundamental roadblocks: nonassociativity of floating-point arithmetic and nondeterminism in the order by which operands are reduced. In this section, we provide an overview of the challenges that arise when nonassociativity collides with nondeterministic reduction. To that end, we discuss the primary mechanisms by which floating-point error arises and propagates. We also summarize the existing body of work addressing issues of nondeterminism at exascale.

##### 2.2.1 Nonassociativity: A Consequence of Finite Precision

Floating-point computations suffer loss of accuracy, compared with the same expression's evaluation in exact arithmetic, through two primary mechanisms: alignment error and subtractive cancellation. Alignment error, by far the most common error modality, results from summation of values whose exponents differ. Alignment error is possible whenever two floating-point numbers that differ in magnitude by at least a



factor of two are added [6]. The amount of information about the smaller operand lost due to alignment error is related to the disparity between the operands’ magnitudes. The other mechanism is subtractive cancellation, which occurs when very small values are obtained from the addition of two values with similar magnitude and opposite sign. Subtractive cancellation, in contrast to alignment error, is not a source of error *per se*, but a means by which inaccuracy in low-order mantissa bits of operands is transferred to high-order mantissa bits of their sum.

A consequence of these inaccuracies is the well-known fact that floating-point arithmetic operations are nonassociative, so the order in which floating-point numbers are reduced via an operator (e.g., +, -, \*, /) influences the result. For example, let  $a = 10^9$ ,  $b = -10^9$ , and  $c = 10^{-9}$ . In infinite precision, the summation orders  $(a+(b+c))$  and  $((a+b)+c)$  are equivalent, but even in double-precision floating-point arithmetic, the two distinct summation orders yield different values.

$$\begin{aligned} ((a+b)+c) &= ((10^9 - 10^9) + 10^{-9}) = 10^{-9} \\ (a+(b+c)) &= (10^9 + (-10^9 + 10^{-9})) = 0 \end{aligned}$$

For a small example such as this one, the flaw is clear, namely, that the small-magnitude value  $c$  is “absorbed” by the much larger value  $b$ .

### 2.2.2 High Concurrency: A Consequence of Extreme Scale

Contemporary petascale platforms consist of up to millions of processor cores that must act in concert to effect large simulations. Even at these scales, the cost of achieving not only accuracy in floating-point reductions but reproducible accuracy is felt. The scientific community at large has set its sights on deployment of an exascale computing platform, and in response the HPC community has identified a canonical set of challenges to implementing an exascale machine [2]. Although emerging developments in low-power hardware, advanced systems software, and algorithm design show promise, it has become increasingly evident that achieving reproducible numerical accuracy at exascale cannot rely on deterministic reduction. Exascale computations

will simply have to weather perturbations in their reduction trees through algorithmic means. In this section, we summarize key results demonstrating how variability in reduction trees induces variability in sums of floating-point numbers. Additionally, we present a set of findings, commentary, and expert recommendations supporting our claim that deterministic reduction trees at exascale will be unfeasible.

Throughout this section and the remainder of the chapter, we adopt the view of a concurrent sum of floating-point numbers at the extreme scale as a *reduction tree*, which we define as a full binary tree whose  $N$  leaf nodes correspond to floating-point operands and whose internal nodes correspond to the partial reductions formed in the process of computing the final result—the root node. Reduction trees can vary in two ways: shape and assignment of operands to leaves. When we refer to the shape of a reduction tree, we mean the particular way in which nodes are linked by edges. Figure 2.1 shows two differently shaped reduction trees: a balanced (parallel) reduction tree and an unbalanced (serial) reduction tree. For a fixed set of operands, even two reduction trees with the same shape can yield different values for the reduction if the assignment of operands to leaves differ between the two trees.

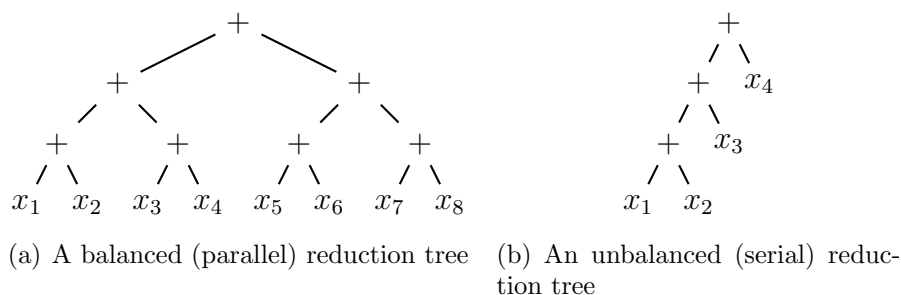


**Figure 2.1:** Two reduction trees at the opposite ends of the spectrum.

The effect of varying reduction tree shape and varying operand-to-leaf assignment is explored in [7]. In their work, a set of eight identical floating-point values is summed via three differently shaped reduction trees, yielding in each case a different value for the sum. Another set of eight floating-point values, six small and two

large, is summed via three reduction trees of the same shape, but with different assignments of summands to leaves. Again, all three computed sums disagreed. One key observation is that the consequences of nondeterministic reduction and floating-point nonassociativity are felt even for extremely small examples.

On exascale systems the high level of concurrency will not allow the user to enforce any specific reduction order because doing so is either too expensive or impossible. At the same time variability in floating-point error accumulation may become so great that debugging is impaired or, worse, fundamentally incorrect results are accepted. An exascale algorithm must exploit the extreme level of concurrency, minimize communication (for speed and power reduction), tolerate frequent hardware failures, and utilize resources as they become available [2], all the while providing some trust in the computation’s result.

The conflict between achieving reproducible accuracy and achieving performance is primarily due to the fact that even on current HPC platforms, communication costs dominate arithmetic costs. Simply put, the most performant reduction trees are those that take into account the underlying physical topology of the system, which means reducing values in an order based on which core produced them, not necessarily their arithmetical properties. Conversely, the reduction trees that result in the least error accumulation reduce values based on their arithmetical properties, not their position in the topology of the system. Recently, Balaji and Kimpe [4] showed not only that topology-aware reduction trees for MPI collective operations outperform fixed-reduction trees but that the performance advantage of allowing the reduction tree to conform to the system topology, as opposed to a specified ordering of partial reduction, increases with the number of cores.

### 2.3 Mathematical Techniques

In response to the challenges posed by the nonassociativity of floating-point summation and the nondeterminism at the extreme scale, mathematical techniques can be applied to mitigate the degree to which computed sums exhibit sensitivity to

reduction order. Lower sensitivity results in increasingly reproducible results. Techniques can range from simple fixed-reduction orders to more sophisticated prerounded algorithms. In this section we provide a general overview of the techniques; however, in the rest of the chapter, we consider only the compensated summation algorithms (Kahan and composite precision) as well as the prerounded algorithms for our studies because they are the only methods that can be feasibly applied at the exascale.

### 2.3.1 Fixed-Reduction Order

To apply fixed-reduction order, we need to ensure that all floating-point operations are evaluated in the same order from run to run. Two major problems exist for this strategy. The obvious problem is that ensuring that the reduction proceeds according to a user-determined reduction tree incurs massive communication and synchronization costs. Additionally, determining exactly which reduction tree achieves minimal error for a given set of summands is nontrivial. Conventional wisdom suggests summing the values in ascending order if they all have the same sign, and in descending order of magnitude if they are not. The first case is rare, however, and the second case assumes that no error beyond initial representation error is present in the summands; otherwise it is far more vulnerable to catastrophic cancellation. In summary, fixing the reduction order is difficult to do correctly where it is possible, but the salient point is that it cannot be done in a cost-effective way at exascale [10].

### 2.3.2 Interval Arithmetic

Techniques based on interval arithmetic replace floating-point types with custom types representing finite-length intervals of real numbers. The actual value of the reduction is guaranteed to lie within the interval. The width of the interval increases with the uncertainty of the computation. While the techniques are reproducible by design, they also cause large slowdown and are not suitable for applications needing many digits of accuracy.

### 2.3.3 High-Precision Arithmetic

Perhaps the most obvious technique, and certainly the most popular in real applications, is to use higher-precision floating-point types. To our knowledge, the earliest work directly addressing the issue of numerical reproducibility [14] demonstrates the use of the double-double precision floating-point type in a critical section of code to curtail variability in a global sum. In that work, the goal of using multiple floating-point types was explicitly to achieve reproducible results. Parallel to that effort, significant progress has been made in the field of automated floating-point precision tuning (e.g., [24]). Precision tuning is an attempt to reduce precision where possible while maintaining a prescribed degree of accuracy. While one can achieve greater reproducibility by pursuing greater accuracy, the use of high-precision arithmetic can result in memory-demanding algorithms. By increasing the size of floating-point variables in most numerically sensitive parts of the algorithm, for example with manual changes made by an expert or by some form of analysis, we can reduce the memory requirements. Still the technique relies on either human experts or other software and thus is probably unsuitable for many of the use cases discussed in the recent DOE exascale report [2].

### 2.3.4 Compensated Summation Algorithms

To compute the sum of  $n$  values, we obtain  $n - 1$  partial sums in the process. For each of these partial sums, the magnitude of error can be estimated. Based on that estimate, an attempt can be made to compensate for that error by adding an error term to each partial sum. Compensated summation is a relatively old technique, having been introduced by Kahan in [17]; but families of more sophisticated compensated summation algorithms have been developed, such as composite precision (CP) summation [28]. In Kahan’s algorithm the estimated error is added back into the sum at each step. In CP, the error summation is kept and propagated as each of the summations are performed and added back in only at the end.

### 2.3.5 Prerounded Summation Algorithms

More recently, an approach called prerounded summation has emerged for reproducible and accurate summation. The common strategy used by this type of algorithm is splitting the operands into “high-order” and “low-order” parts with the property that the high-order parts can be summed irrespective of summation order and the low-order parts can be neglected, or recursed upon, for higher accuracy. The algorithms proposed by Demmel and his group are integrated into the ReproBLAS library [11], which at this time is undergoing active development.

## 2.4 Inadequacy of Conventional Wisdom

The management of reproducible numerical accuracy is closely related to the task of estimating and predicting error accumulation. Three common approaches exist, typically used in isolation, to quantify and mitigate error accumulation. Two of the approaches can be broadly classified as techniques for error estimation: using worst-case error bounds and attempting to track or avoid subtractive cancellation. The third approach is the use of summation algorithms that are believed to be inherently less sensitive to variability in the reduction tree. We emphasize that these approaches have significant value. However, we demonstrate that the use of any one approach, in isolation, will not guarantee the reproducibility desired without a potentially significant loss of performance.

### 2.4.1 Using Analytical Error Bounds

The analysis of the error for a single floating-point sum can be extended to produce a worst-case error bound for the reduction of multiple floating-point values. For IEEE-compliant implementations of floating-point arithmetic, we have the following bound on the roundoff error for a single operation. Let  $x, y$  be floating-point numbers, let  $\text{fl}(x + y)$  be their rounded sum according to a given rounding rule, and let  $(x + y)$  be their exact sum:

$$\text{fl}(x + y) = (x + y) \cdot (1 + \delta)$$

where  $|\delta| \leq u$  where  $u$  is the unit-roundoff and may be written  $u = \frac{1}{2}\beta^{1-p}$ , where  $\beta$  is the base and  $p$  is the number of mantissa bits of the representation of  $x$  and  $y$ . Equivalently, if we let  $z$  denote the exact sum  $x+y$ , we obtain a bound on the absolute error  $|\text{fl}(x+y) - z| \leq u$ . With some algebra, one can prove an upper bound on the error in a sum of  $n$  floating-point numbers. We do not include the proof here (it may be found in [15]), but we state the result. Let  $x_1, \dots, x_n$  be floating-point numbers, let  $z$  denote their exact sum, and let  $\sum_{i=1}^n x_i$  denote their sum in floating-point arithmetic. Then we have the following upper bound on the absolute error in the sum:

$$\left| \sum_{i=1}^n x_i - z \right| < n \cdot u \cdot \sum_{i=1}^n |x_i|.$$

Using analytical or statistical worst-case error bounds causes overestimation of the errors. Figure 2.2 shows an empirical case study in which we measure the error magnitudes for 10,000 values sampled in the range  $(-1000, +1000)$  and summed by using 10,000 different summation orders. The figure also shows both the analytical and statistical worst-case error bounds. Both error bounds significantly overestimate the error magnitude. At the same time we observe the large range of measured errors obtained for the same set of values just by randomly shuffling the order in which the terms are summed.

#### 2.4.2 Tracking Cancellations

When considering sets of summands with both positive and negative values, the potential for *catastrophic cancellation* arises in the computation of the sum. This numerical phenomenon can result in large relative errors in both the partial and final sums, leading to the intuitively appealing perspective of achieving reproducible accuracy by structuring reductions to avoid cancellation.

Cancellation in general refers to the scenario where the sum of two floating-point values has a smaller exponent than both of the summands. In order to subtract one floating-point number from another, their binary points are aligned and the mantissa of their difference is determined by subtracting the mantissas of the operands bitwise

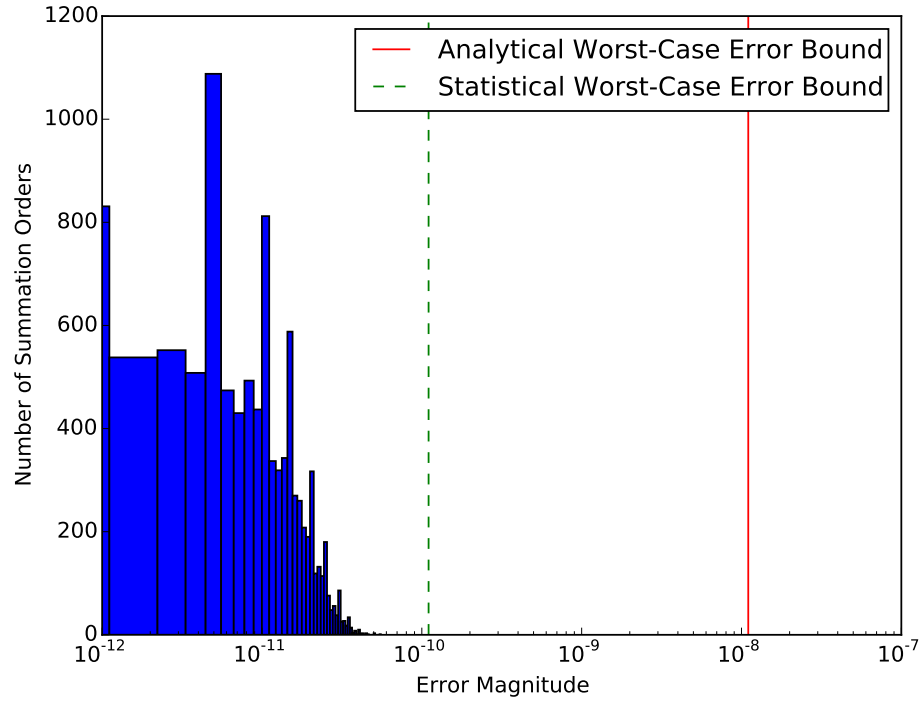


**Figure 2.2:** Empirical study of error magnitudes and worst-case error bounds for 10,000 summations of 10,000 values randomly sorted.

and then *renormalizing* the result. The effect of the renormalization process is that the lower-order bits of the operands determine the higher-order bits of the result. If both summands are exact in the sense that their mantissa bits are not carrying the error from previous computations—as is almost never the case—then their difference can be considered accurate. However, if the low-order bits of the operands are inaccurate due to alignment error, many or all of the mantissa bits of the difference of the operands may be inaccurate. This is the “catastrophic” case.

We emphasize, however, that cancellation does not in and of itself cause error to accumulate. Rather, it reveals error that has already accumulated in the operands. In a sense, relative error can increase because of catastrophic cancellation as uncertainty in less-significant bits of the operands’ mantissas is transferred to uncertainty in the most significant bits of the result’s mantissa. Nevertheless, the number of cancellations is not a reliable indicator of the overall problem.



To prove this claim, we generate a counterexample with a set of 1,000 floating-point numbers uniformly distributed in  $[-1, 1]$ . We compute the sum of these numbers using 100 distinct summation orders and determine the error for each order. We assess cancellation for each order using the numerical library CADNA [16]. CADNA uses the CESTAC method to identify instances of cancellation in a sum and, for each instance, estimate the difference between the number of accurate digits in the operands and the number of accurate digits in the result. In this sense, a cancellation resulting in the loss of four digits of accuracy is more severe than a cancellation resulting in the loss of only two digits. Figure 2.3 shows the cancellation counts and error magnitudes for several summation orders of the set of interest for our counterexample. Each summation order is represented by five bars, four showing the number of cancellations resulting in the loss of one, two, four, and eight digits, respectively, and a fifth bar showing the error magnitude, scaled for ease of viewing. We observe that the number of cancellations, at any of the considered severities, does not consistently predict error magnitude. In particular, consider summation orders 2 and 4. Order 2 has about 5X as many digit cancellations as order 4, but only half the error. This result lends credence to the view that although it is tempting to view “keeping track of cancellations” as a valid strategy for managing error and ensuring reproducibility, there is not a simple correspondence between instances of cancellation and error magnitude. Rather, the relationship between cancellation and error depends on knowledge of how much error has already accumulated in the operands involved in the cancellation, a quantity whose estimation is impeded by the previously discussed loose error bound.

### 2.4.3 Choice of Summation Algorithm

Apart from the standard iterative summation algorithm, we examine other summation algorithms that exhibit reduced sensitivity to variability in the reduction tree. However, each of these algorithms incurs a certain performance penalty relative to the standard summation. Standard summation is the cheapest and least complex. Kahan’s compensated summation, then composite precision summation, and finally

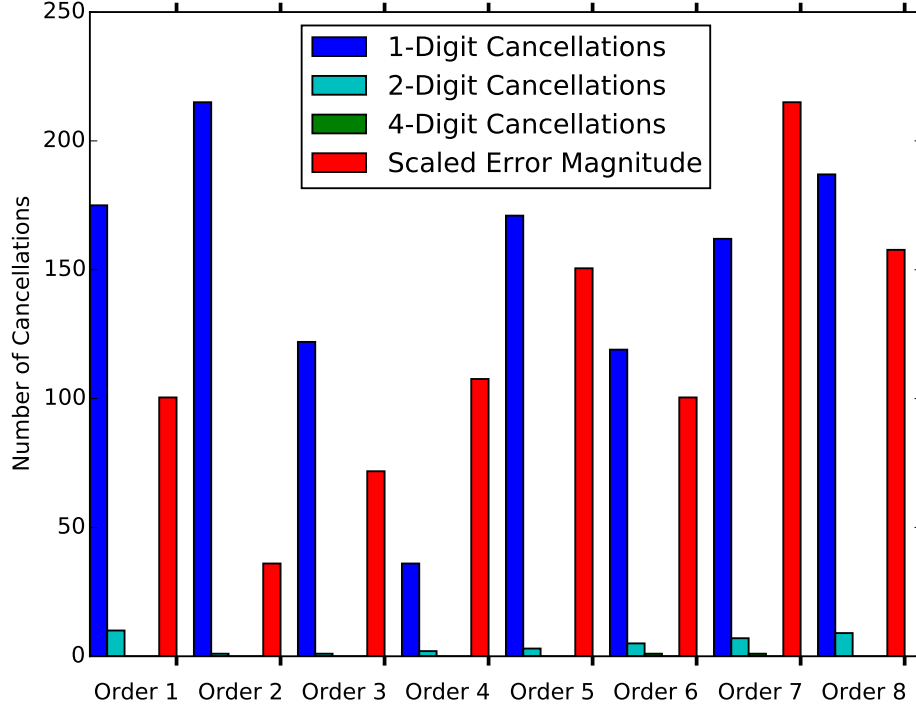


**Figure 2.3:** Empirical study of cancellations vs. error magnitude for different summation orders.

prerounded summation are expected to progressively provide more accuracy at the expense of performance. To assess this performance impact, we measure the execution times of a case study designed to emulate scenarios in scientific computing in which partial data is locally generated on multiple processes and then is globally reduced across the processes. Specifically, on each process, we generate a chunk of a vector of values of length  $10^6$  from a series that is known to sum to zero under exact arithmetic. We locally reduce these values using each of the four summation algorithms: in the case of Kahan and composite precision, we use the summation operators in [23] and in the case of prerounded summation, we use the `dIAddd` operator provided in [22]. Finally, we globally reduce the local sums by using `MPI_Reduce` with custom reduction operators for Kahan, composite precision, and prerounded summations. To avoid time variations due to network contention we run our tests on a single dedicated 48-core AMD node. Each tests is repeated 20 times with a warmed cache. Figure 2.4 shows

the average execution times and Figure 2.5 shows the performance penalties associated with more-reproducible summation. The latter figure confirms the proposed ranking of the summation algorithms in terms of performance expense.

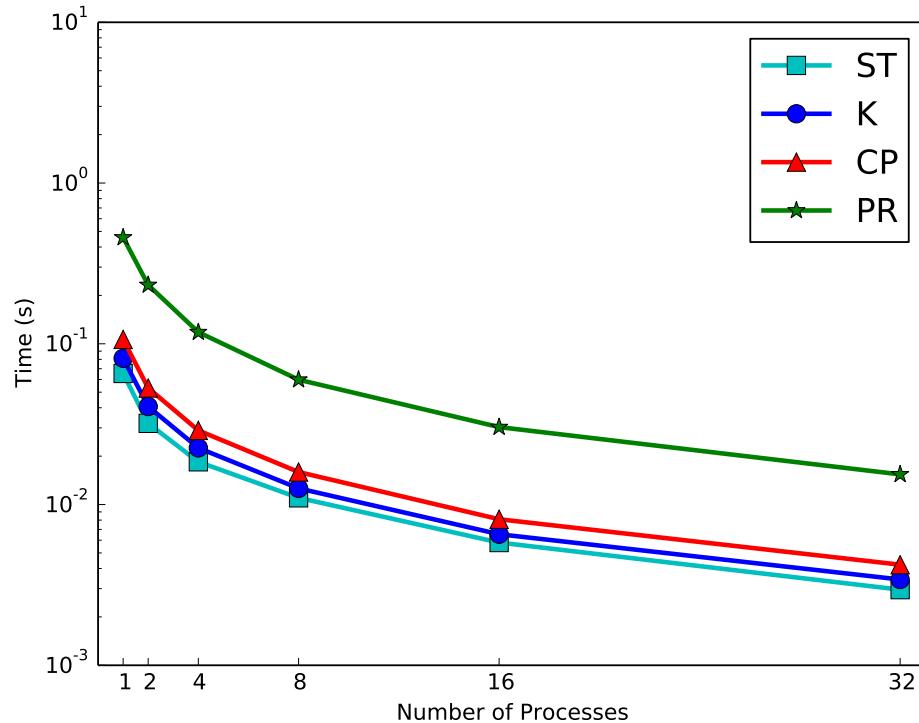


**Figure 2.4:** Comparison of execution time to sum  $10^6$  terms for standard summation (ST), Kahan’s compensated summation (K), composite precision summation (CP), and prerounded summation (PR).

We argue that applying a judicious mixture of these algorithms, as opposed to uniformly applying a single technique, is necessary for achieving numerical reproducibility to the degree required by an application, for a cost acceptable for that application. Figures 2.6(a) and 2.6(b) support this claim by showing the relative sensitivity of the three summation algorithms: Kahan’s compensated summation (K), composite precision summation (CP), and prerounded summation (PR). For a fixed set of data we generate multiple reduction trees of the same shape but with different assignments of operands to leaves. We construct the set of summands to have mathematical properties that render its reduction especially prone to both alignment error and loss of

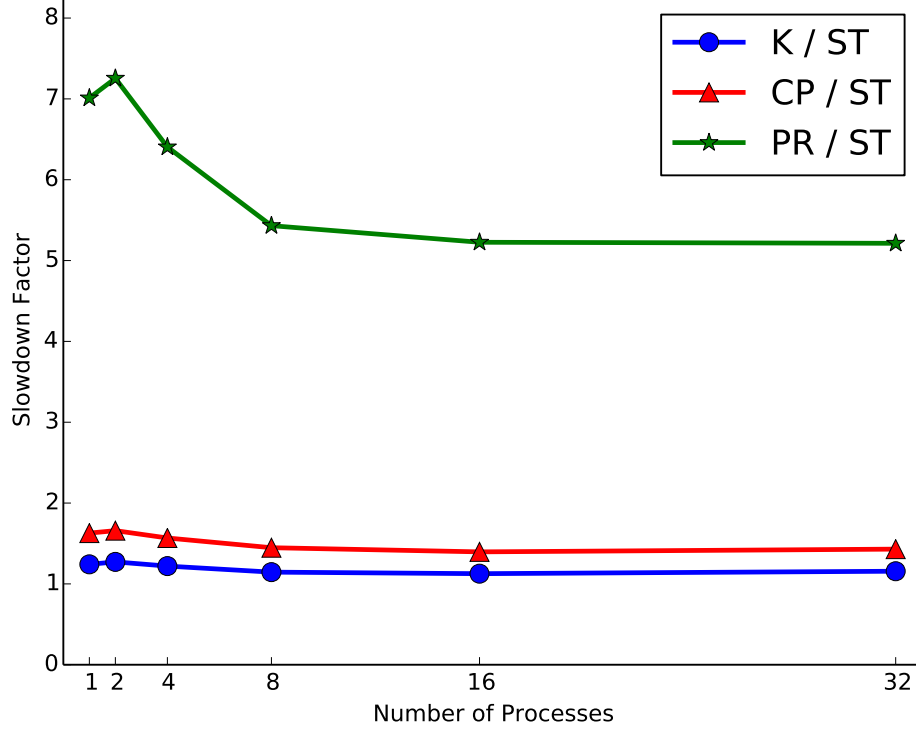


**Figure 2.5:** Performance losses of Kahan’s compensated summation (K), composite precision (CP), and prerounded (PR) summations compared to the standard summation (ST).

accuracy due to cancellation. For each reduction tree, we compute the sum using each of the four algorithms. By plotting the error magnitude, we see that as a progressively greater amount of computation is invested in compensating for roundoff error, the sum becomes less sensitive to the varying reduction tree.

## 2.5 Exploring the Reproducibility Space

Previous work [7, 4] found that reduction tree shape and assignment of operands to its leaves (or threads) can have a profound effect on the concurrent sum of  $n$  floating-point numbers, even when the operands themselves are subject to minimal alignment error and have the same sign avoiding cancellation. We build the work in this chapter on this previous work by targeting a much larger reduction scale and investigating the impact of four independent parameters on the variability of a sum when the reduction

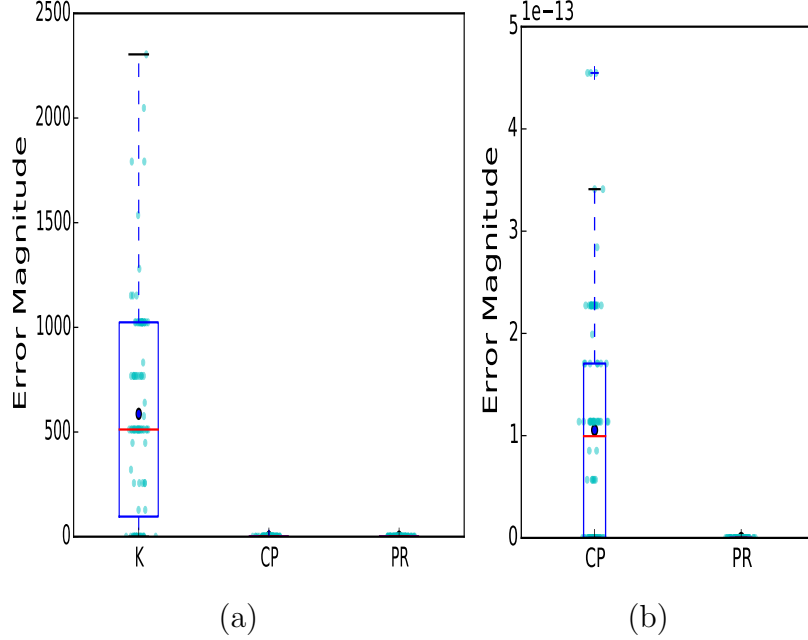


**Figure 2.6:** Empirical study of relative sensitivity of three summation algorithms: Kahan’s compensated summation (K), composite precision summation (CP), and prerounded summation (PR). Note that (a) zooms into (b).

order is non-deterministic. The four parameters we consider are the condition number, the dynamic range, the level of concurrency, and the reduction algorithm. We present three kinds of results. First, we examine the sensitivity to variations in the reduction tree of four summation algorithms at increasing levels of concurrency. Second, we study the impact of concurrency, condition number, and dynamic range on reproducible numerical accuracy. Third, we provide evidence of the need for selecting application-aware reduction algorithms.

### 2.5.1 Experimental Environment and Parameters

Building on the results of small nondeterministic reduction trees established in [7, 20], we consider reduction trees at the size expected for exascale systems consisting of floating-point operands reflective of those actually reduced in simulations. Since an exascale system is not available, we emulate the reduction process with  $n$  threads, each computing one of the  $n$  partial sums. We consider two tree shapes at

opposite ends of the spectrum: a completely balanced (see Figure 2.1(a)) tree and a completely unbalanced (see Figure 2.1(b)) tree. For each tree shape, we generate distinct reduction trees by randomly assigning operands to leaves. We also focus on sets of floating-point summands whose mathematical properties are less amenable to reproducible summation. We characterize sets of floating-point values by their sum condition number and dynamic range. These are intrinsic properties of the set of values; they are independent of any imposed ordering. For a set of floating-point numbers  $\{x_1, \dots, x_n\}$ , the sum condition number is defined as

$$k = \left( \sum_{i=1}^n |x_i| \right) / \left| \sum_{i=1}^n x_i \right|$$

and the dynamic range is defined as

$$dr = \exp(\max(|x_i|)) - \exp(\min(|x_i|)),$$

where  $\exp(x)$  is the value of the exponent in the representation of  $x$ . If the dynamic range of two numbers is larger than zero, then alignment error will occur. For this reason, we use the dynamic range of a set of values as a rough estimator of alignment error. The condition number does not correspond to a single mechanism by which error accumulates. Instead, it describes how sensitive the final sum is to small errors in the partial sums.

Table 2.1 shows small sample sets of values presenting dynamic range  $dr$  equal to 0, 8, and 16 as well as condition number  $k$  equal to 1, 1000, and  $\infty$ . Note that  $dr$  equal to 0 means “all exponents are the same” and not that the numbers are large or small; on the other hand a larger  $dr$ , for example 8 or 16, means that a larger discrepancy exists between the largest and smallest exponents. In other words, the sign on the summands makes no difference, and the sum of summands makes no difference. A condition number equal to 1 means “all values in sum have the same sign,” while a condition number infinity means “the sum of all the values is 0.” In [7] the operands are well-conditioned; they have  $k = 1$  (the best possible condition number) and, when varying tree shape, have  $dr = 0$ . We instead focus on ill-conditioned inputs with high

**Table 2.1:** Example of sample set of values with specified dynamic range,  $dr$ , and condition number,  $k$ .

Sample Set of Values	$dr$	$k$
$\{1.23\text{e}+32, 1.35\text{e}+32, 2.37\text{e}+32, 3.54\text{e}+32\}$	0	1
$\{1.23\text{e}-32, 1.35\text{e}-32, 2.37\text{e}-32, 3.54\text{e}-32\}$	0	1
$\{-1.23\text{e}+16, -1.35\text{e}+16, -2.37\text{e}+16, -3.54\text{e}+16\}$	0	1
$\{2.37\text{e}+16, 3.41\text{e}+8, 4.32\text{e}+8, 8.14\text{e}+16\}$	8	1
$\{3.14\text{e}+32, 1.59\text{e}+16, 2.65\text{e}+18, 3.58\text{e}+24\}$	16	1
$\{2.505\text{e}+2, 2.5\text{e}+2, -2.495\text{e}+2, -2.5\text{e}+2\}$	0	1000
$\{5.00\text{e}+2, 4.99999\text{e}-1, 1.0\text{e}-6, -4.995\text{e}+2\}$	8	1000
$\{5.00\text{e}+2, 4.99\ldots99\text{e}-1, 1.0\text{e}-14, -4.995\text{e}+2\}$	16	1000
$\{3.14\text{e}+8, 1.59\text{e}+8, -3.14\text{e}+8, -1.59\text{e}+8\}$	0	$\infty$
$\{3.14\text{e}+4, 1.59\text{e}-4, -3.14\text{e}+4, -1.59\text{e}-4\}$	8	$\infty$
$\{3.14\text{e}+8, 1.59\text{e}-8, -3.14\text{e}+8, -1.59\text{e}-8\}$	16	$\infty$

dynamic range because reality is not so rosy. For example,  $N$ -body simulations [3] involve reductions of floating-point values that are ill-conditioned; both  $k$  and  $dr$  can frequently be very large.

### 2.5.2 Sensitivity of Summation Algorithms

To examine the sensitivity of summation algorithms to variability in the reduction tree, we generate and reduce two sets of summands constructed to have the exact sum of zero and dynamic range of 32. One set has  $n = 8K$  values, and the other has  $n = 1M$  values. These sets of values are more prone to both alignment error and catastrophic cancellation than are those studied in [7]. They are also more reflective of the values that may arise in simulations (e.g., when the net force on a particle is close to zero).

Figures 2.7(a)–(h) show the distribution of error magnitudes for sums computed by using varying reduction trees for the four summation algorithms of interest in this chapter: the standard iterative summation algorithm (ST); Kahan’s compensated summation algorithm (K); the composite precision summation (CP), which can be considered an enhanced form of compensated summation; and the prerounded summation (PR), which offers guaranteed bitwise reproducibility at a user-specified level of

accuracy. We consider two types of reduction trees: completely balanced, with results shown in Figures 2.7(a), (b), (c), and (d), and completely unbalanced, with results shown in Figures 2.7(e), (f), (g), and (h). For each tree type, we consider both smaller levels of concurrency (8K leaves in the tree) and higher levels (1M leaves in the tree). The boxplots in the figures are obtained by considering 100 distinct reduction trees with the same shape but randomly permuted assignments of the values to leaves. Note that Figures 2.7(b), (d), (f), and (h) provide a zoom-in into Figures 2.7(a), (c), (e), and (g), respectively.

The effect of nondeterminism in the reduction tree is exhibited in Figures 2.7. For a given summation algorithm, the distribution of data points and width of the box indicate how much the sum tends to vary when the overall shape of the reduction tree is constant but the arrangement of summands to its leaves is variable. Within the subfigures, we see that although Kahan summation tends in general to produce more reproducible sums than standard summation, only composite precision and prerounded summations offer reproducible numerical accuracy at an acceptable level. Across a row of subfigures, we see that as the level of concurrency rises, the absolute error in the sum rises as expected. However, by comparing results across a column of subfigures, for example, the ST data from Figure 2.7(a) and the ST data from Figure 2.7(e), we see that much more variation in the sum occurs when the tree is unbalanced than when it is balanced for the standard summation algorithm. To cope with intermittent faults and inconsistently available resources, we expect that the reduction trees employed by an exascale system will vary not only in terms of arrangement of data among their leaves but also in overall shape. We conclude that because of the difference in reproducibility observed for differently shaped reduction trees, exascale applications will need to maintain awareness of the degree of fluctuation in reduction tree shape and employ more robust reduction operators accordingly.



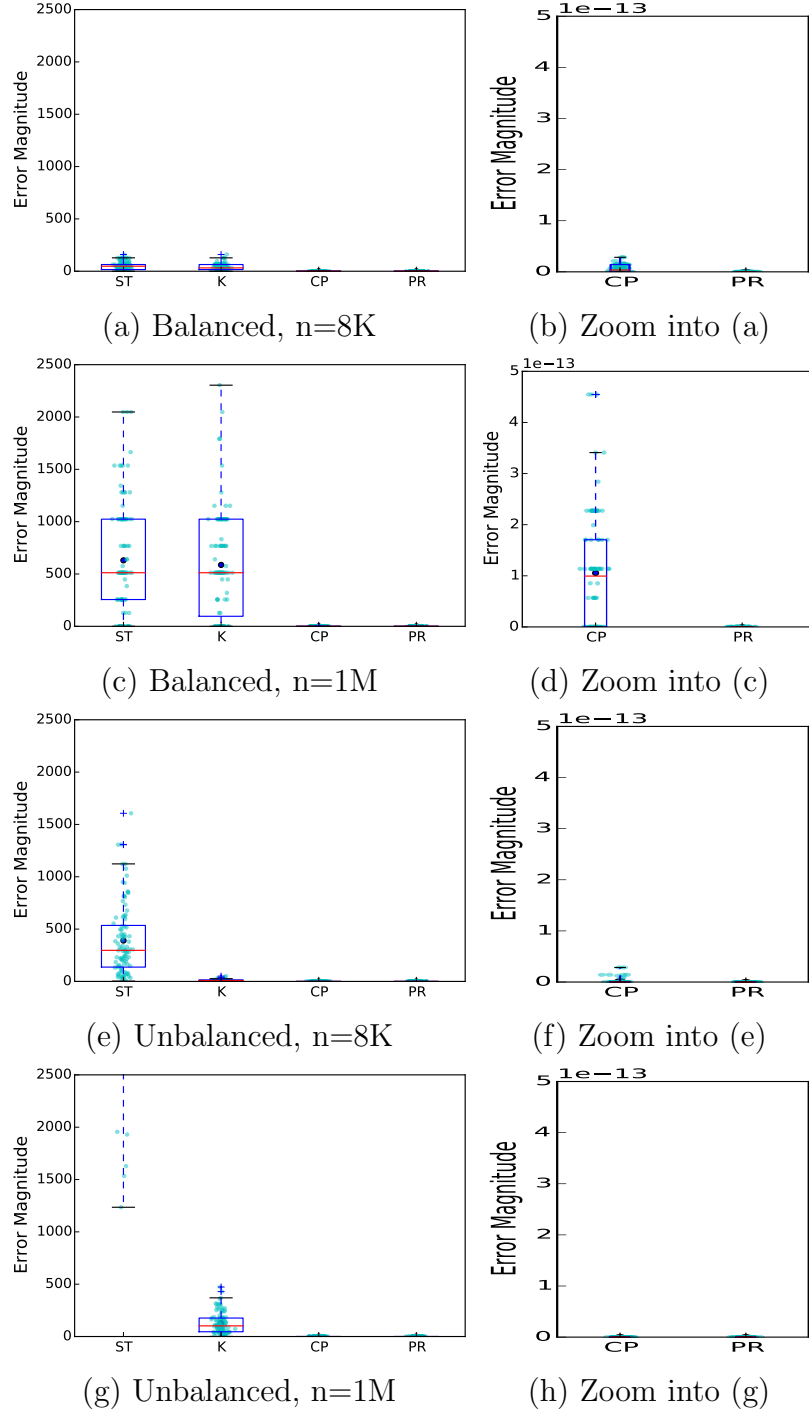


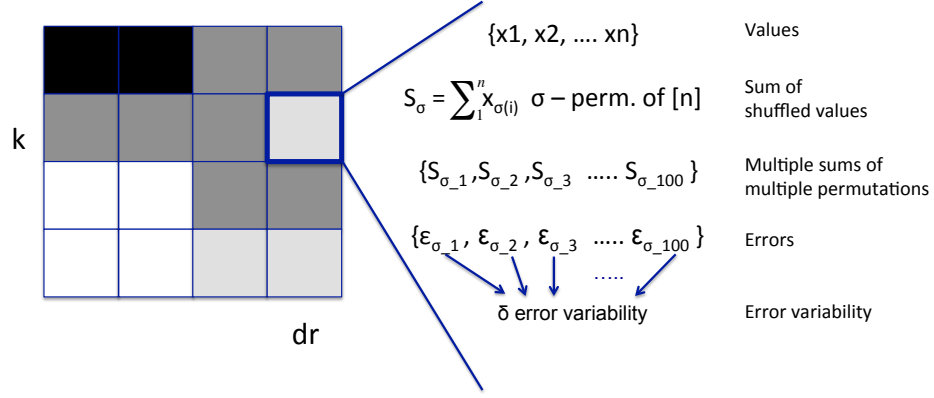
**Figure 2.7:** Error distributions for the four summation algorithms considered in this chapter for balanced and unbalanced reductions: three at a smaller (8K leaves) and one at higher (1M leaves) levels of concurrency.

### 2.5.3 Effect of Concurrency, Conditioning, and Dynamic Range

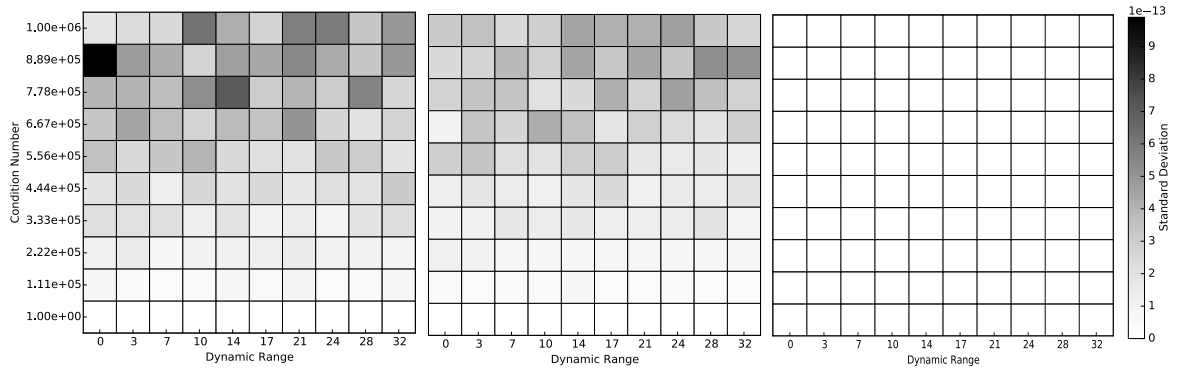
For a fixed level of concurrency, the mathematical properties of the summands can have a significant impact on the sensitivity of the sum to variations in the reduction tree. In the previous section, we considered a set of values with a fixed condition number  $k$  and dynamic range  $dr$ . In this section, we examine the effects of varying  $k$  and  $dr$  at a fixed level of concurrency  $n = 1M$ ; varying  $dr$  and  $n$  at a fixed  $k$ ; and varying  $k$  and  $n$  at a fixed  $dr$ . We represent the spaces of  $(k, dr)$ ,  $(n, dr)$ , and  $(n, k)$  as a grid of cells, where for each cell we generate a set of floating-point values with the cell parameters. The degree to which these sets of values can be summed reproducibly is tested. For all sets of summands under consideration, we measure their potential for irreproducibility by computing their sum with 1,000 distinct, balanced reduction trees obtained by permuting the assignment of summands to leaves. As in our previous experiment we test four summation algorithms. However, we display results only for the first three because the composite precision and prerounded summations performed identically for all sets of inputs considered. Once all the sums have been computed for a cell, the error in each sum is calculated with respect to an accurate reference sum, which we compute in quad-double precision using the GNU MPFR high-precision library. To visualize the level of irreproducibility observed, we compute the standard deviation of the errors and shade the cell according to that value. Figure 2.8 illustrates the process in a visual (and more intuitive) way.

Figure 2.9 shows how position in the space of possible  $(k, dr)$  values influences the variability of a sum at a fixed level of concurrency. The darker cells toward the top and right of the two leftmost grids indicate sets of summands whose sums varied much more than the level of variation observed for sets of summands with lower condition number. The darkest cell in the standard summation grid is anomalous but likely due to particularly severe subtractive cancellation, since its condition number is large. The rightmost grid shows that for all considered sets of summands, the result according to the composite precision summation did not vary with changes in the reduction tree.

Figure 2.10 presents the impact of dynamic range for a fixed condition number.



**Figure 2.8:** Overview of the grid with its cells used to study the effect of concurrency, conditioning, and dynamic range.



**Figure 2.9:** Standard deviation errors for standard summation (left), Kahan summation (middle), and composite precision summation (right) for different  $(k, dr)$  values and fixed concurrency  $n$ .

For these grids, each cell's summands have condition number  $k = 1$  so that the ability of dynamic range to estimate alignment error can be assessed. Note that the scale by which the cells are shaded for these grids is not the same as for the grids examining the  $(k, dr)$  or  $(n, k)$  spaces. There is a tendency for high-concurrency, high-dynamic-range cells to exhibit greater variability; but the most valuable lesson from these visualizations is that dynamic range exerts much less influence over variability of the sums than does the condition number, as seen in Figure 2.11. Here, we observe a strong relationship between high variability of sums and sets of summands with high condition

number. These results suggest the need for applications to maintain awareness of the mathematical properties of sets of floating-point values generated at runtime, and if the reduction tree is expected to change from run to run, to select reduction algorithms that take those mathematical properties into account.

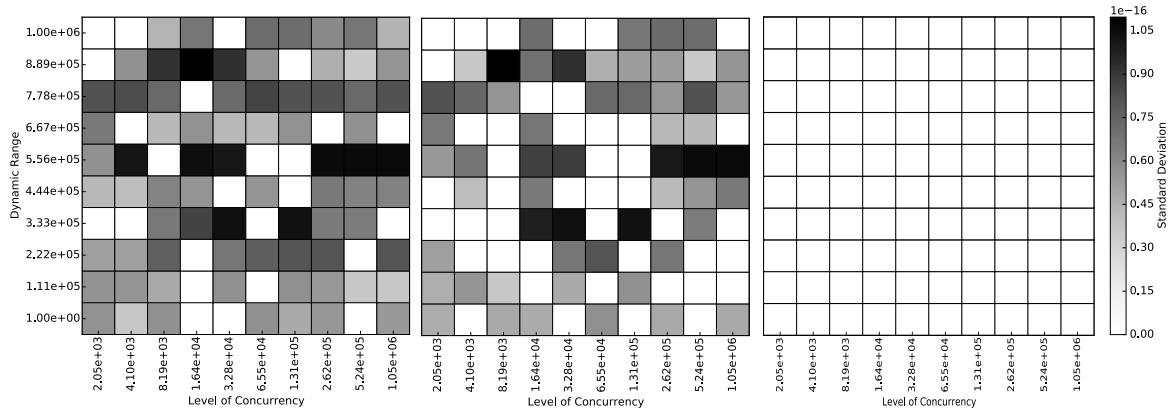


**Figure 2.10:** Standard deviation errors for standard summation (left), Kahan summation (middle), and composite precision summation (right) for different  $(n, dr)$  values and fixed condition number  $k$ .

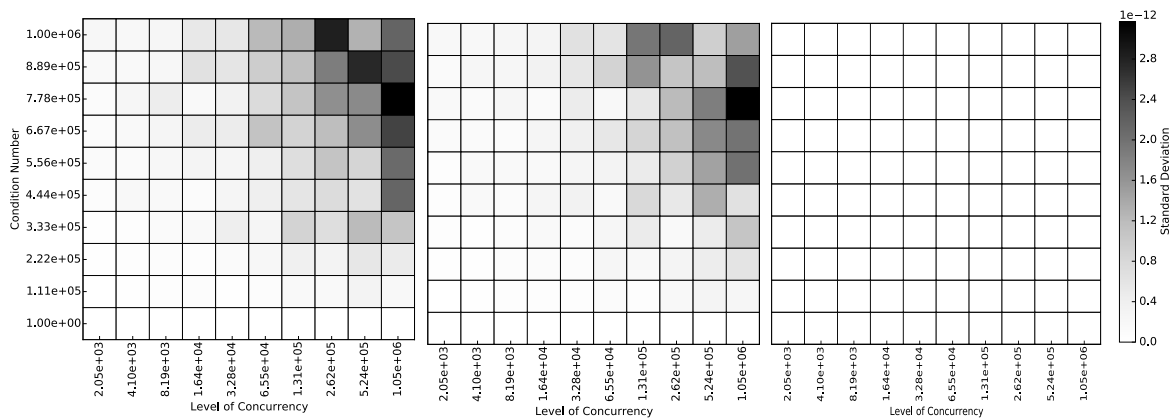


**Figure 2.11:** Standard deviation errors for standard summation (left), Kahan summation (middle), and composite precision summation (right) for different  $(n, k)$  values and fixed dynamic range  $dr$ .

#### 2.5.4 Intelligent Selection of Reduction Algorithms

Techniques such as compensated summation can reduce the amount of variability observed in repeated summation when the summation order changes from run to run. However, application developers are faced with the challenge of selecting the summation algorithm that gives them the level of reproducibility and accuracy required by their application. At exascale, judicious selection of reduction algorithms will be vital so that application-specific reproducible numerical accuracy can be achieved at tolerable cost. In contrast to the old notion of bitwise reproducibility, application-specific reproducibility requires developers to specify an upper bound on the amount of variability in the values of floating-point reductions that can be tolerated while maintaining the trustworthiness of the application’s output.

A set of floating-point values occupies a position in a complex parameter space: the number of values, reduction tree, condition number, and dynamic range all exert influence over which reduction algorithm can cost-effectively achieve a specified level of reproducibility. Our data suggests that in order to avoid exceeding a fixed level of variability, if one cannot control the reduction tree, it may be possible to use standard summation when values are uniform and well-conditioned and to adaptively switch to a more robust summation algorithm if the values to be reduced become less uniform or less well-conditioned. We argue that unlike attempting to achieve reproducible numerical accuracy by additional data movement, as would be required to fix a reduction tree, estimable quantities such as condition number and dynamic range can guide runtime selection of a reduction operator with the appropriate performance/reproducibility tradeoff for the application at hand. In Figure 2.12, we show the  $(k, dr)$  grid for several error variability thresholds. Here cells are shaded based on the cheapest summation algorithm that achieves a given degree of reproducibility at that cell. As we reduce the variability threshold, effectively stepping toward bitwise reproducibility with smaller and smaller thresholds, we see that increasingly costly summation algorithms are required for the more challenging regions in the space (i.e., those with high condition number and high dynamic range).

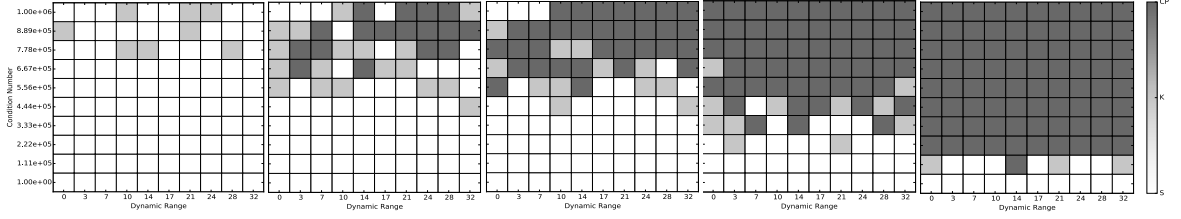


**Figure 2.12:** Selection of the cheapest but acceptably accurate reduction algorithm among the Kahan (K), composite precision (CP), and prounding (PR) algorithms for different error variability thresholds (left to right:  $t = 5e - 13, 3e - 13, 2.5e - 13, 1.5e - 13, 5e - 14$ ).

Achieving reproducible numerical accuracy by intelligent runtime selection of reduction algorithms depends on being able to assess the mathematical properties of the floating-point values to be reduced. We show that if this assessment can be done, one can avoid using a more expensive reduction algorithm when a cheaper one will do. These results present a strong case for further research into tools that, at exascale, profile parameters of interest (e.g.,  $n$ ,  $k$ ,  $dr$ , and tree shape) at runtime and apply cheaper but acceptably accurate reduction algorithms to subtrees based on the profile.

## 2.6 Lessons Learned

In this chapter we tackle the first of our two challenges (i.e., the numerical challenge). We identify relevant parameters that, when analyzed in concert, can provide insight into intelligent selection of reduction algorithms to achieve reproducible numerical accuracy on soon-to-exist exascale platforms.

Three main observations emerge from our study on reproducible numerical accuracy. First, reduction tree shape has a large impact on reproducible numerical accuracy. Second, mathematical properties of a set of summands have an impact on the reproducibility of their sum. In applications where the conditioning and dynamic range can change dramatically over the course of the runtime, this effect is especially relevant. Third, we show that if we fix a target level of reproducibility, we can classify regions of

the parameter space by the cheapest algorithm that achieves the desired level of reproducibility at that point in the space. This is an important step toward implementing intelligent runtime selection of reduction operators on future exascale platforms.

## Chapter 3

### THE DEBUGGING CHALLENGE

#### 3.1 Introduction

In this chapter we first provide an overview of the record-and-replay approach for debugging a class of non-deterministic applications and describe the properties of existing record-and-replay tools. We then present our extension to the record-and-replay approach together with the performance of the integration of our extension into a production-grade record-and-replay tool.

#### 3.2 Record-and-Replay Approach and Tools

To overcome the impediments to debugging associated with non-deterministic executions, a class of debugging aids collectively referred to as record-and-replay tools have been developed. These tools allow developers to record one execution of a target application, then replay it exactly. In general, record-and-replay tools must establish an order of events during the recorded execution, then write a representation of that order to some form of persistent storage. The exact data that must be recorded depend on what assumptions can be made about the form of nondeterminism the target application exhibits. Figure 3.1 shows a general overview of these tools' framework.

Necessary behaviors of record-and-replay tools can be sorted in two groups: during recording and during replay. During recording, a tool must observe communication events in an application's execution and store (or write) information that unambiguously orders the observed events into a record. One way to do this task is with logical clocks and metadata (described in the next section). Metadata in message passing applications include processes' rank, tag, and communication event type (e.g., completion of a receive vs. invocation of Test-family function).



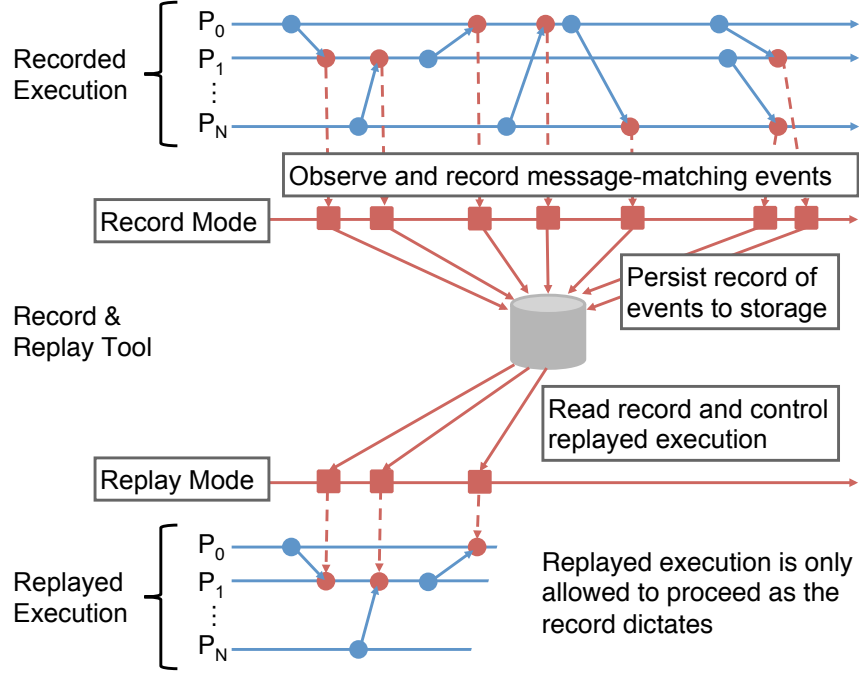


**Figure 3.1:** General overview of a record-and-replay framework.

During replay, a tool must read (or query) the record followed by buffering and re-ordering communication events in the subsequent execution. Correctness of the replay depends on assumptions about the application (e.g., is the application send-deterministic) [5] and inductive arguments (e.g., the  $n^{th}$  event is replayed correctly as a consequence of the  $n - 1^{th}$  event being replayed correctly).

Existing record-and-replay tools fall into two broad categories: data-replay and order-replay. These categories refer to the content that is traced by the tool during recording. Specifically, data-replay tools record the total content of messages, whereas order-replay tools opt instead to record the messages' relative ordering. The state of the art in record-and-replay takes the order-replay approach primarily due to the significant reduction in record size it provides by not recording possibly large message payloads in addition to the necessary message order data.

The earliest record-and-replay tools employed the data-replay approach, but

attempt to mitigate the growth of record size via selectively recording only those messages deemed at runtime to be a source of non-determinism. Netzer and Miller employ vector clocks to identify racing messages and thus restrict the number of necessarily recorded messages in their tool [21]. Later work by Clémecq *et al.* used a similar vector clock approach, but extended the tool’s capabilities to record non-blocking probes as well as wildcard receives [8]. Despite these techniques’ applicability at the time of their creation, their use of vector clocks makes them prohibitively expensive for modern HPC systems, since each message is saddled with a vector of  $n$  elements where  $n$  is the number of processors in the system [13].

Later record-and-replay tools embraced the order-replay design, recognizing that despite the need to make stronger assumptions about message contents than data replay tools do, increasingly large systems necessitate the smaller record sizes that order-replay tools can deliver. One early tool in this domain was the Nondeterministic Program Evaluator (NOPE) developed by Kranzlmüller and Volkert [18]. Last, Clock-Delta Compression (CDC) [25] is the state-of-the-art approach to record-and-replay that aims to overcome the problem of large record size that renders traditional record-and-replay techniques inapplicable at extreme scale. We build our work on top of this approach that we describe in the next section.

### 3.3 Clock-Delta Compression

Clock-Delta Compression (CDC) establishes an order on communication events during recording by piggybacking logical clocks on messages between processes, and applies a novel compression pipeline to the record that leverages properties of the piggybacked clocks. In this section, we provide an overview of the CDC record format, a high-level description of the compression pipeline, and describe the role of the piggybacked logical clocks with respect to the record format and the compression pipeline.

The CDC record format is a data structure built up during recording that contains sufficient information about interprocess communication events to enable deterministic replay of the recorded execution. The record format consists of three main

parts: the *with-next-table*, the *unmatched-test-table* and the *matched-test-table*. The *with-next-table* records when multiple incoming messages match with a single receive request, as can occur if `MPI_Testsome`, `MPI_Testall`, `MPI_Waitsome`, or `MPI_Waitall` are employed by the application. The *unmatched-test-table* records instances of `MPI_Test`-family functions being called on a receive request when no matching send exists, as can occur when a polling loop of test calls is used to complete a non-blocking receive. Finally, the *matched-test-table* records the actual matches between receive requests and incoming messages. This component of the record format is our focus since the most dramatic reductions in record size that CDC offers apply to the *matched-test-table*. Moreover, the specific implementation of the underlying logical clock protocol directly effects the compressibility of the *matched-test-table*.

The CDC compression pipeline is applied to the CDC record format during recording and consists of three stages: permutation encoding, linear-predictive encoding (LPE), and lossless compression. The permutation encoding stage is applied only to the *matched-test-table*, whereas LPE is applied to components of the *matched-test-table* and *unmatched-test-table*. The lossless compression stage is applied to the entire record after permutation encoding and LPE. We provide the description of the algorithm for permutation encoding in Section 3.6 due to the critical reduction in size of the *matched-test-table* that it provides and the degree to which its functionality is intertwined with the notion of a logical clock ticking policy described in Section 3.4.

### 3.4 Logical Clocks

Logical clocks, originally defined by Lamport in [19], provide a method for establishing a partial order on events in a distributed system. Within the context of the CDC record-and-replay technique, we describe the rules of the logical clock protocol that CDC employs, we define the notion of logical clock ticking policy, and we discuss how recording events are distinguished by the logical clock values associated to them.

CDC establishes a partial order on all communication events that occur during recording by maintaining in each process  $p$  an integer value referred to as the local clock

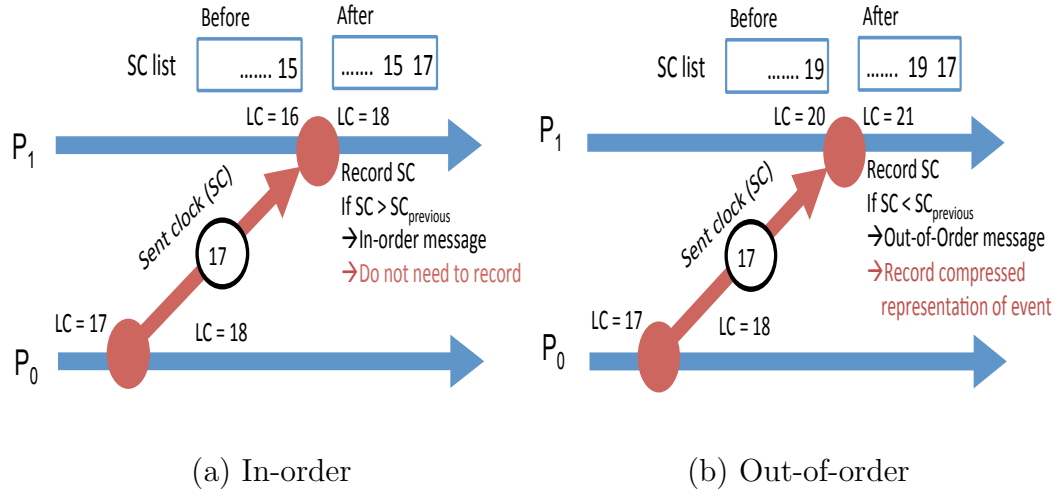
of that process. Whenever  $p$  sends a message to another process,  $p$  attaches a copy of its local clock to the message, then increments its local clock by some value  $t$ , hereafter referred to as a “tick”. When another process  $q$  receives  $p$ ’s message, it sets its own local clock to the maximum of its current value and the value attached to the message it just received. Then  $q$  increments its local clock by some amount (i.e.,  $q$  ticks its local clock). Two immediate consequences of this protocol are that within a process, if an event  $e_0$  occurred before another event  $e_1$ , the logical clock values associated to those events (e.g.,  $c_0$  and  $c_1$ ) satisfy  $c_0 < c_1$ , and between a sender process and a receiver process, a send event’s clock will always be less than its corresponding receive event’s clock.

So far we have discussed logical clocks’ ticks without specifying what values they must take. In Lamport’s paper on logical clocks [19], ticks are assumed to always equal 1, but in fact all that is necessary to establish a partial order is that the ticks have positive value. In the context of record-and-replay, since the replayed execution must exactly match the recorded execution, we require the additional constraint that the ticks be deterministic (i.e., during replay), for all processes, the  $i$ th tick applied to a process’s local clock must match the  $i$ th tick that was applied to its local clock during recording. We define a *logical clock ticking policy* to be a mechanism for deciding what value each tick applied to each process’s logical clock will take.

### 3.5 In- and Out-of-order Received Messages

In this section, we define the concept of an event (e.g., message receive) being in-order or out-of-order with respect a logical clock reference order, and how out-of-order messages impact the size of the *matched-test-table*. In CDC, every receive completion event is associated to a logical clock value that is piggybacked on a received message. Specifically, each process has a “local clock” (LC) that is initially zero. When a process (e.g.,  $P_0$ ) sends a message, its LC is attached to the message as the “sent clock” (SC). Afterward, the sending process’s LC is incremented by one. When a process (e.g.,  $P_1$ ) receives a message from another process (e.g.,  $P_0$ ), it updates its LC by the Lamport

Clock protocol  $LC = \max(LC, SC) + 1$  and records the receive event. The list of SC values that every receiving process builds up over the course of recording an execution defines whether a received message is in-order or out-of order: if the new SC is larger than the previous received SC, then the message is in-order; if it is smaller, then the message is out-of-order. The SC values are the input to the permutation encoding step of the CDC compression pipeline, and the degree of monotonicity in this list of values determines the effectiveness of the compression. Moreover, the list of SC values is not the same logical clock value that any receiving process updates its local clock to, and as such does not impose a partial order on events in the same way. Figure 3.2 shows examples of in-order or out-of-order messages: Figure 3.2.(a) shows an example of an in-order received message and Figure 3.2.(b) shows an example of an out-of-order received message. In Figure 3.2.(a), the SC of  $P_0$  is 17; because the SC value is larger than the previous SC of  $P_1$  (in the figure the  $SC_{previous}$  is 15), the received in-order message is annotated in the SC list but will not be recorded in the *matched-test table*. This is not the case in Figure 3.2.(b) in which the SC of the sending  $P_0$  is still 17 but the previously annotated SC is larger (i.e., equal to 19), causing the recording of the event in the *matched-test table*.



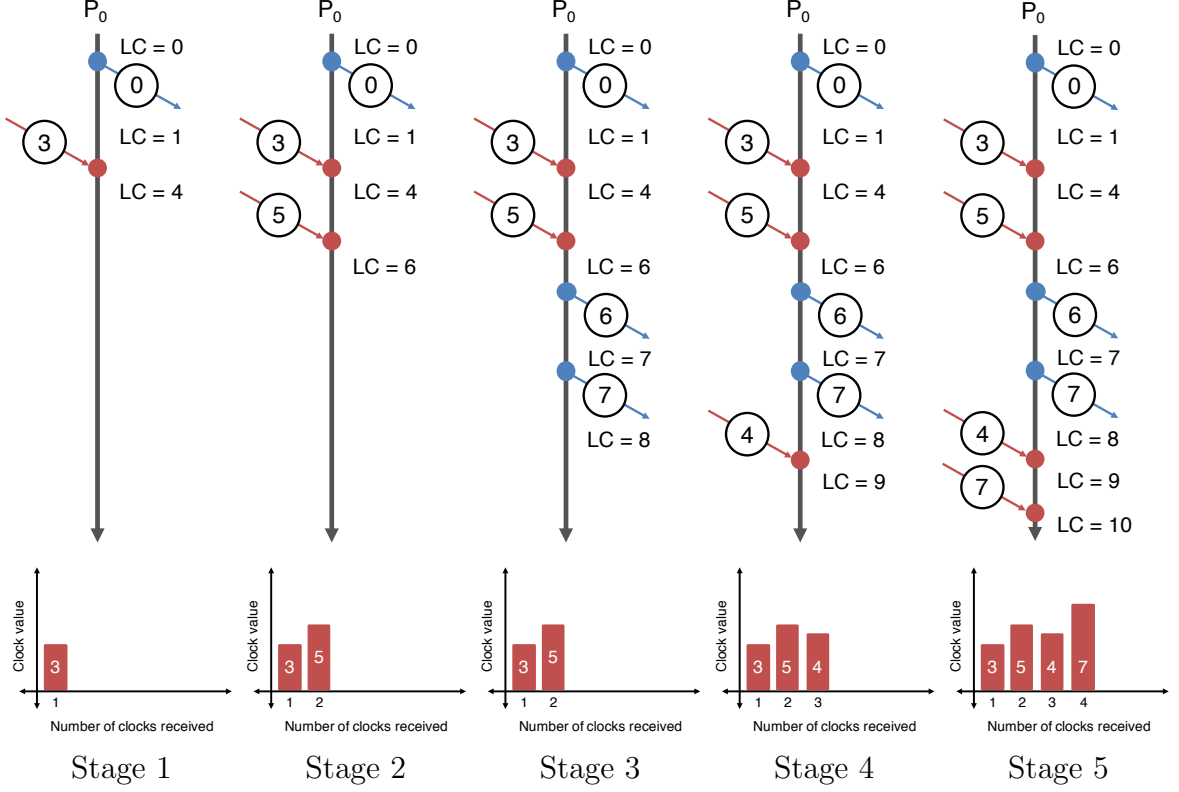
**Figure 3.2:** Example of in-order (a) and out-of-order (b) messages.

Figure 3.3 show a larger five-stage example in which multiple messages are received by a process  $P_0$ . For each stage, the upper figure shows the snapshot with the sent and received messages up to that point for process  $P_0$ ; the bottom figure shows the associated SC list. In Stage 1,  $P_0$  receives a message from, for example,  $P_1$ .  $P_0$  updates its local clock (LC), which was initially equal to 1, by using the Lamport Clock protocol to 4 (i.e., LC of  $P_0$  becomes the max of LC and SC plus one) and temporally records the time of the received message (i.e., SC time is equal to 3). In Stage 2,  $P_0$  receives a second message from  $P_2$ ;  $P_0$  updates its LC following the same procedure as in Stage 1. The LC of  $P_0$  becomes 6 and the process also records the received SC value (in this case SC is equal to 5). We observe that at the end of Stage 2 the received clocks' values are monotonically increasing "in-order". The process takes note of the message's SC but does not forward the SC value to its *matched-test table*. In Stage 3,  $P_0$  sends messages. Its LC increases each time a send is initiated but no clock is recorded. In Stage 5, two additional messages from a different process than  $P_1$  are received by  $P_0$ . This time the first message is out-of-order (i.e., with a SC equal to 4 smaller than 5) and is thus used for building the process' *matched-test table*. The second is in-order (i.e., with a SC equal to 7 larger than 4) and is not considered for the process' *matched-test table*.

### 3.6 Permutation Encoding

During recording, the process receiving messages with the attached logical clock values builds up the *matched-test table*. The table collects only information on out-of-order messages and therefore, the number of out-of-order messages determines the size of the *matched-test table*.

Sato *et al.* made the observation that for most processes, the list of received clock values tended to consist of values that were nearly-sorted in increasing order (i.e., in-order messages), as show in the authors' manuscript [25]. The observed similarity between the actual order of received clock values (referred to hereafter as the observed order) and the ordering of received clock values in ascending order (referred



**Figure 3.3:** Example of a five-stage execution in which in-order and out-of-order messages are received by process  $P_0$ . We show in-order receives in stages 1, 2, 3, and 5. We show an out-of-order receive in stage 4, in which a sent clock of 4 is received after  $P_0$  has already received a larger sent clock of 5.

to hereafter as the logical clock reference order) suggests that there is a compact way of representing the difference between the observed order and the reference order. This difference, which can be thought of as the permutation that maps the reference order to the observed order, is what the permutation encoding stage computes. Representing the *matched-test table* by this permutation suffices for replay because during replay, messages arriving in arbitrary order can be buffered, sorted based on their piggybacked logical clock values into the reference order, and then *un-sorted* into exactly the observed order from recording by applying the recorded permutation.

The permutation encoding stage works by computing a minimal set of edits that effectively map the logical clock reference order back to the observed order. Each edit

is represented as a pair of integers (i.e., an index and an offset). Consider that if a process receives all its inbound messages such that their piggybacked logical clock values are received in strictly ascending order, then the observed order and the logical clock reference order are identical (i.e., all messages are received in-order). Since permutation encoding is an effective compression technique to the extent that the observed order is similar to the logical clock reference order, a reduction in the number of out-of-order message receives translates to a reduction in the size of the *matched-test table*, and consequently a reduction in the size of the total record. Figure 3.4 shows how, for the example in Figure 3.3, we need to swap only the 2nd and 3rd message receives to create our observed sequence of messages starting from a totally in-order set of message. Therefore, “swap(2,3)” is written to the *matched-test table* for  $P_0$  and everything else is discarded.

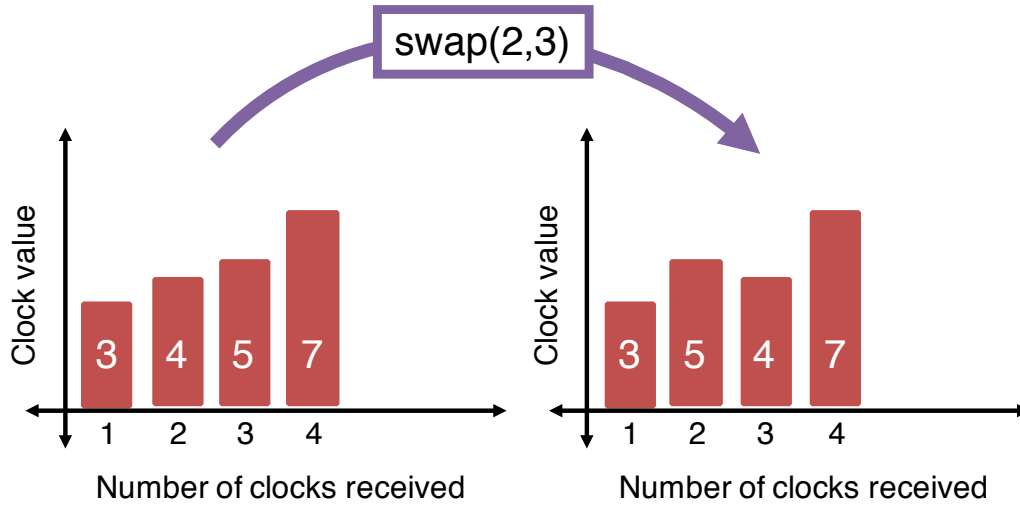


**Figure 3.4:** Process to transform a totally in-order set of message receives into the order we observed for Figure 3.3.

During the replay stage, a record-and-replay tool buffers incoming messages and re-orders them so that the processes receive the messages in the same order the processes did during the recorded execution. Figure 3.5 shows the steps followed by the replay stage for the example in Figure 3.3.



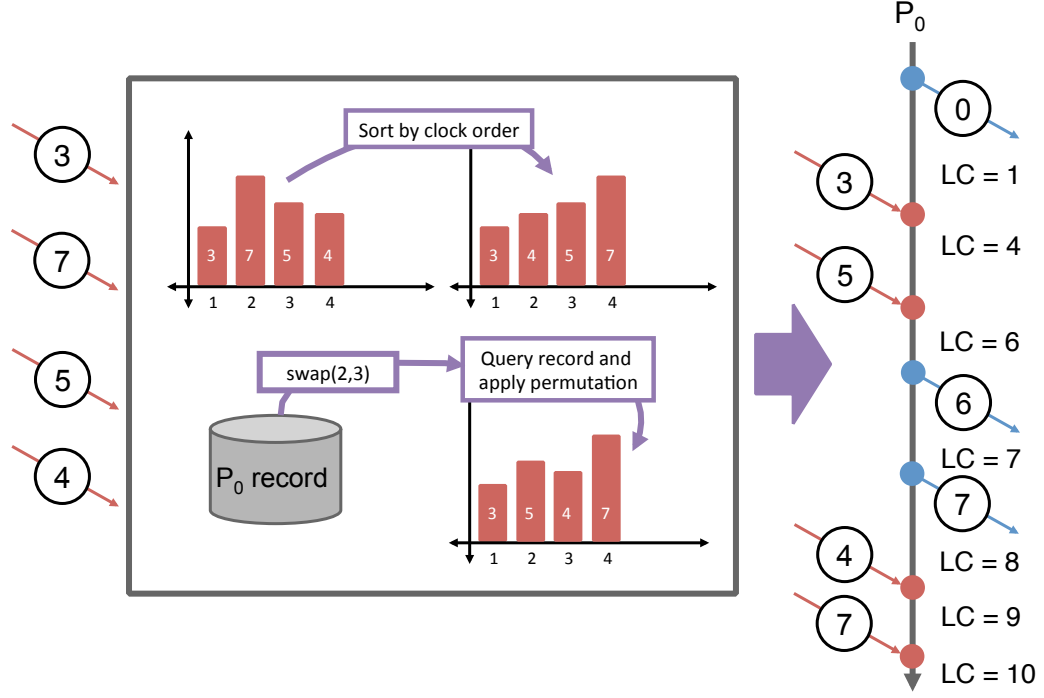


**Figure 3.5:** Steps performed by the replay stage in a record-and-replay tool to recreate the observed execution built during the record stage.

### 3.7 Logical Clock Ticking Policies

To minimize the size of the matched-test table, and hence the size of the overall record, it is necessary to minimize the number of messages that are received out-of-order. Sato *et al.* propose to accomplish this minimization by means of a logical clock ticking policy designed to accurately reflect the number messages received. This policy that we call “basic ticking” ticks by 1 each time a message reception is completed, as shown in Figure 3.6.(a).

In an ideal recording scenario, all messages arrive at their receiving processes such that their attached clock values are received in ascending order. In light of this, it is tempting to attempt to implement a ticking policy based on wall-time values, as depicted in Figure 3.6.(b). However, such a ticking policy cannot provide deterministic ticks, and hence causes incorrect replay. Nevertheless, we integrated this policies in Sato’s record-and-replay tool ReMPI and we collected data on the rate of out-of-order

messages observed under a wall-time based ticking policy to investigate the degree to which a specialized ticking policy can improve over the baseline policy of setting each tick equal to 1. As we will show below, empirical investigation indicates that a ticking policy that matches closely with wall-time based ticking but retains replayability can reduce the rate of out-of-order messages, and hence reduce the size of the matched-test table.

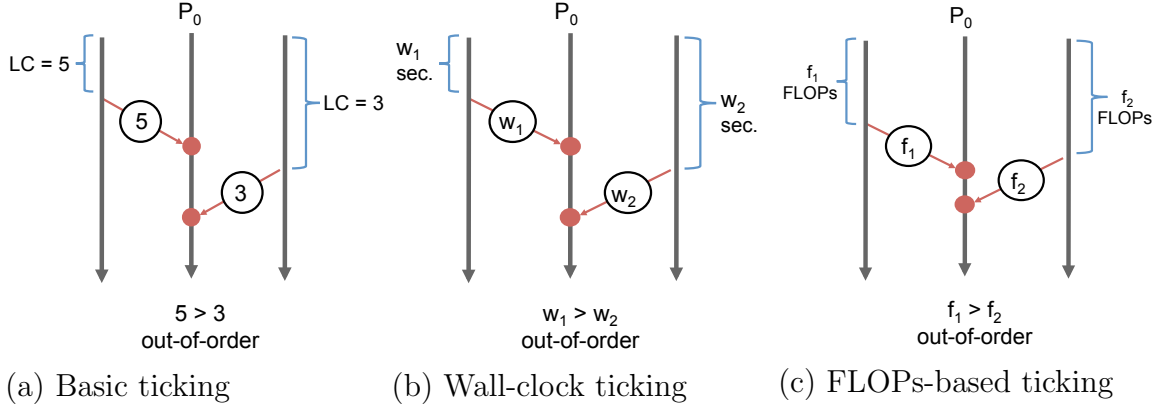


**Figure 3.6:** High level overview of the three ticking policies considered in this work: (a) basic ticking, (b) wall-clock ticking, and (c) FLOPs-based ticking.

In the message-passing HPC applications that record-and-replay tools target, processes often alternate between progressing through intensive floating-point workloads and communicating with other processes. As such, we propose a FLOPs-based ticking that uses the number of floating-point instructions completed by a process as a proxy for wall-time. We use the Performance Application Programming Interface (PAPI) to monitor floating-point instructions completed, and derive ticks from those values. Empirical investigation not shown in this thesis indicates that the PAPI\_FP\_INS performance counter, which measures floating-point instructions completed, yields deterministic values, and hence deterministic ticks, when limited to counting floating-point instructions at the application level exclusively. We use the MPI profiling interface (PMPI) to intercept MPI function calls made by applications and halt PAPI's counters until control returns to the application, as shown in Figure 3.6.(c).

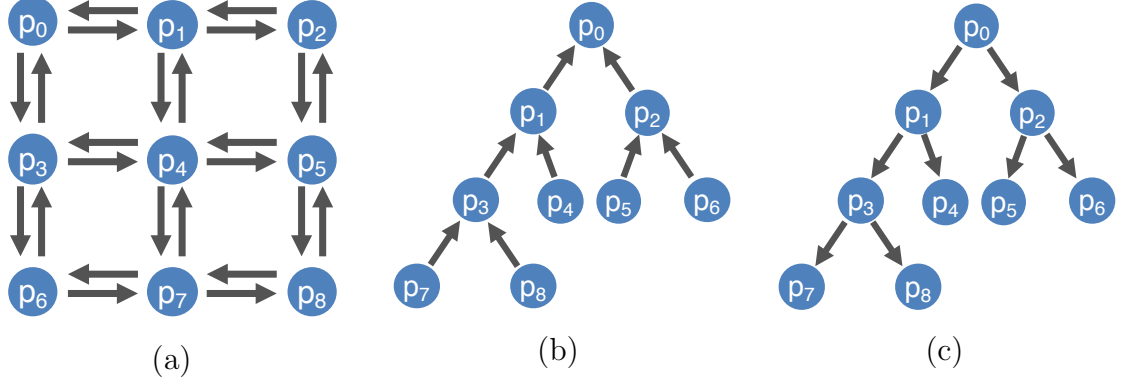


**Figure 3.7:** MCB communication patterns: the neighbor-to-neighbor particle exchange (a), the non-blocking gather (b), and the non-blocking scatter (c).

### 3.8 Applicability to Real Applications with Real Record-and-Replay Tool

To evaluate the effectiveness of our PAPI.FP\_INS-based ticking policy in reducing the rate of out-of-order message receives, we record multiple executions of a representative message-passing application, the Monte Carlo Benchmark (MCB) [1], with a record-and-replay tool that implements CDC, called Reproducible MPI (ReMPI) [25]. In this section, we provide our rationale for evaluating our ticking policy using MCB and ReMPI.

MCB is an MPI application that simulates particle dynamics in a domain that is decomposed over a set of MPI processes. Particles that exit one process’s subdomain are buffered and subsequently sent to a neighbor process’s subdomain via non-blocking point-to-point communication. MCB progresses its simulation by alternating between three distinct communication patterns, as shown in Figure 3.7. The three patterns are: neighbor-to-neighbor particle exchange where processes communicate with their neighbors in a Cartesian grid; non-blocking gather where processes are organized into a binary tree topology and send messages to their parents in the tree; and non-blocking scatter where processes are once again organized as a binary tree, but the direction of communication is from parent to child. MCB is known to exhibit non-deterministic

communication due to its use of non-blocking point-to-point communication and wildcard receives (i.e., allowing a pending receive request to match with the first message that arrives), rather than a message from a specific sender. Moreover, run-to-run variability in MCB’s numerical outputs has been observed [9] that is attributable to non-deterministic communication. Consequently, MCB is an ideal candidate application for testing a record-and-replay tool.

We implement our ticking policies in ReMPI. ReMPI is, to the best of our knowledge, the only record-and-replay tool that implements CDC. Additionally, ReMPI’s design as a composition of PMPI modules [12] [27] simplified the implementation of our ticking policy. By default ReMPI uses the basic ticking policy where all ticks are set to 1.

### 3.9 Assessing Different Ticking Policies

We compare our ticking policy based on floating-point operations against the baseline ReMPI ticking policy. In our analysis we consider the effect of application-level parameters (i.e., floating-point workload per process and rate of messaging between processes) on the rate of out-of-order messages.

#### 3.9.1 Experimental Setting

By varying the number of particles that each MPI process initially simulates, we can effectively vary the intensity of each process’s floating-point workload (i.e., the more particles are simulated per process, the more floating point operation are performed). Note that we consider a homogeneous distributed of particles per process. By varying the size of the communication buffer between two processes each process uses to accumulate particles en-route to a neighbor process, we can effectively vary the rate of communication (i.e., by decreasing the buffer size we increase the number of messages issued). In Figure 3.8 we show the four scenarios we test in this thesis (in green). We consider either 1K or 1M particles for process and either a buffer size

containing data for 5 or for 5,000 particles leaving a process subdomain for the neighbor process sharing the buffer.

		MCB Message Buffer Size ( Smaller == More Messages )			
		5	50	500	5000
# Particles per Subdomain ( Larger == More FLOPs )	1K				
	10K				
	100K				
	1M				

**Figure 3.8:** Tested scenarios (in green cells) in the space of application parameters considered in this thesis. Gray cells are left for future work.

For each one of the four MCB scenarios we evaluate our FLOPs-based ticking (referred in the figures in the next section as PAPI\_FP\_INS-ticking) against the baseline ticking policy built into ReMPI (hereafter referred to as MPI\_SEND-ticking) and a non-replayable wall-time-based ticking policy (referred to as MPI\_WTIME-ticking). For each scenario and each ticking policy, we record 100 executions of MCB with the extended ReMPI set to log the number of messages received in-order and the number of messages received out-of-order by each MPI process. For each process, we compute the percentage of messages received out-of-order, and then aggregate these percentages across all 100 executions, thereby obtaining a global view of the ticking policies’ effectiveness at minimizing the rate of out-of-order messages.

We conduct our tests on Vulcan, a BlueGene/Q cluster at Lawrence Livermore National Laboratory. Each node of Vulcan consists of 16 1.6 GHz PowerA2 processors and is equipped with 16 GB of RAM. The nodes are networked to each other in a 5D torus. We consider three scenarios consisting of one single node running a 16-processes

MCB, four nodes running a 64-processes MCB, and 16 nodes running a 256-processes MCB.

### 3.9.2 Results

Figures 3.9 plot the distributions of out-of-order message percentages for each ticking policy and the median out-of-order percentage for each ticking policy over all executions on a single node of Vulcan. At the single-node scale, we observe that

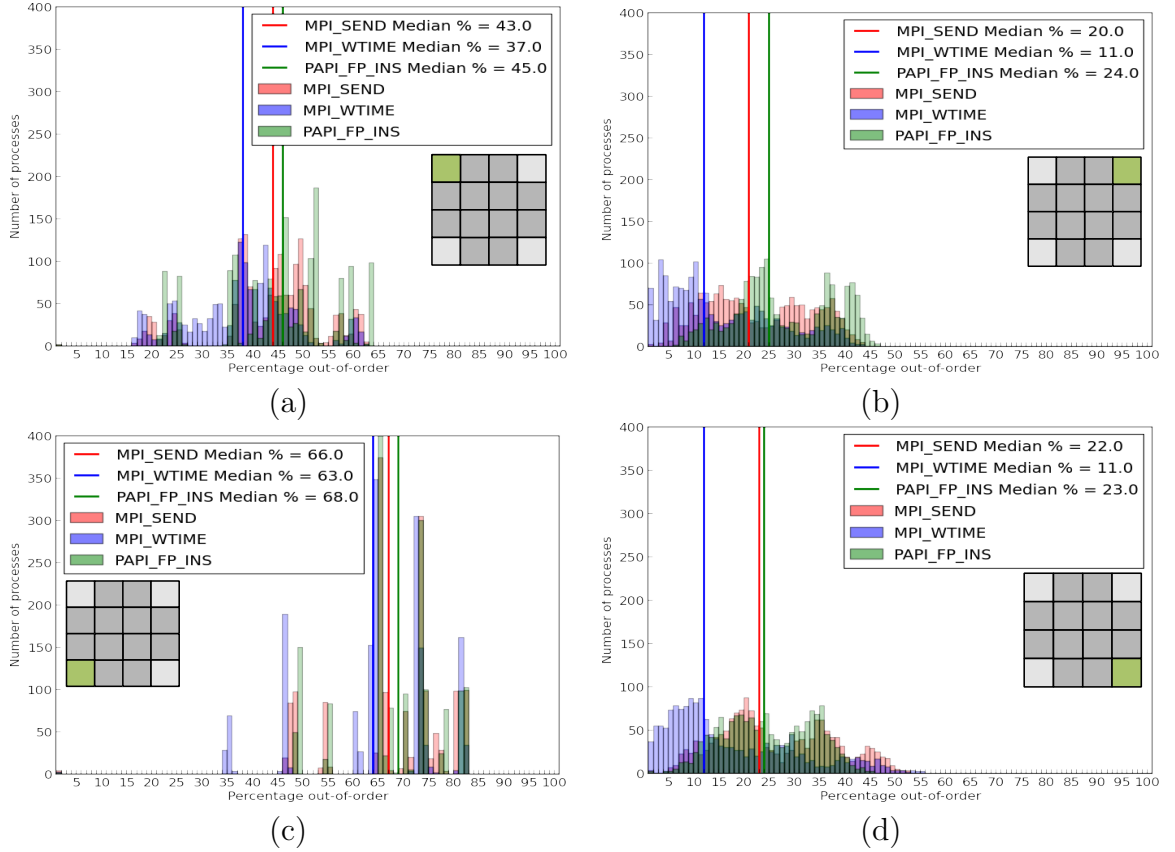


**Figure 3.9:** Distributions of out-of-order message percentages and median out-of-order percentage for each ticking policy over all executions on a **single node** of Vulcan. The test cases are: 1K particles per process, buffer size 5 (a); 1K particles per process, buffer size 5K (b); 1M particles per process, buffer size 5 (c); and 1M particles per process, buffer size 5K (d).

MPI\_WTIME-ticking improves the median out-of-order message percentage relative

to MPI\_SEND-ticking best when communication intensity is low (i.e., when the MCB buffer size is large). The median improvement is 9% in the low floating-point workload case, and 11% in the high floating-point workload case. Conversely, when the communication intensity is high due to a small MCB buffer size, the improvement MPI\_WTIME-ticking offers is minimized—6% and 3% respectively. We conjecture that this is due to the fact that when more messages are sent per unit of wall-clock time, ticking by 1 per message send more closely resembles the passage of wall-clock time than in the case where message sends are less frequent. In all four cases however, we note that the PAPI\_FP\_INS-based ticking does not improve the median out-of-order percentage relative to MPI\_SEND-ticking, contrary to our expectation. We do note however that in the low communication intensity and high floating-point workload case, the out-of-order message rate of PAPI\_FP\_INS-ticking closely approaches that of MPI\_SEND-ticking.

In the four-node tests shown in Figures 3.10, we observe that while MPI\_WTIME-ticking continues to excel in the low communication intensity cases, MPI\_SEND-ticking matches it very closely in the high communication intensity cases, even slightly exceeding it when the per-process floating-point workload is also low. Also notable is that in the two high floating-point workload cases, PAPI\_FP\_INS-ticking matches very closely with MPI\_SEND-ticking, lending further credence to the idea that PAPI\_FP\_INS-ticking can be useful for applications where per-process floating-point workload strongly influences the timing of message sends.

At the 16-node scale shown in Figures 3.11, we observe that even in the low communication intensity, low floating-point workload case, MPI\_SEND-ticking gets very close to the performance of MPI\_WTIME-ticking. The trend we have so far observed of strong agreement between all three ticking policies in the high communication intensity, high floating-point workload case continues, as does the trend of strong agreement between MPI\_SEND-ticking and PAPI\_FP\_INS-ticking in the low communication intensity, high floating-point workload case.

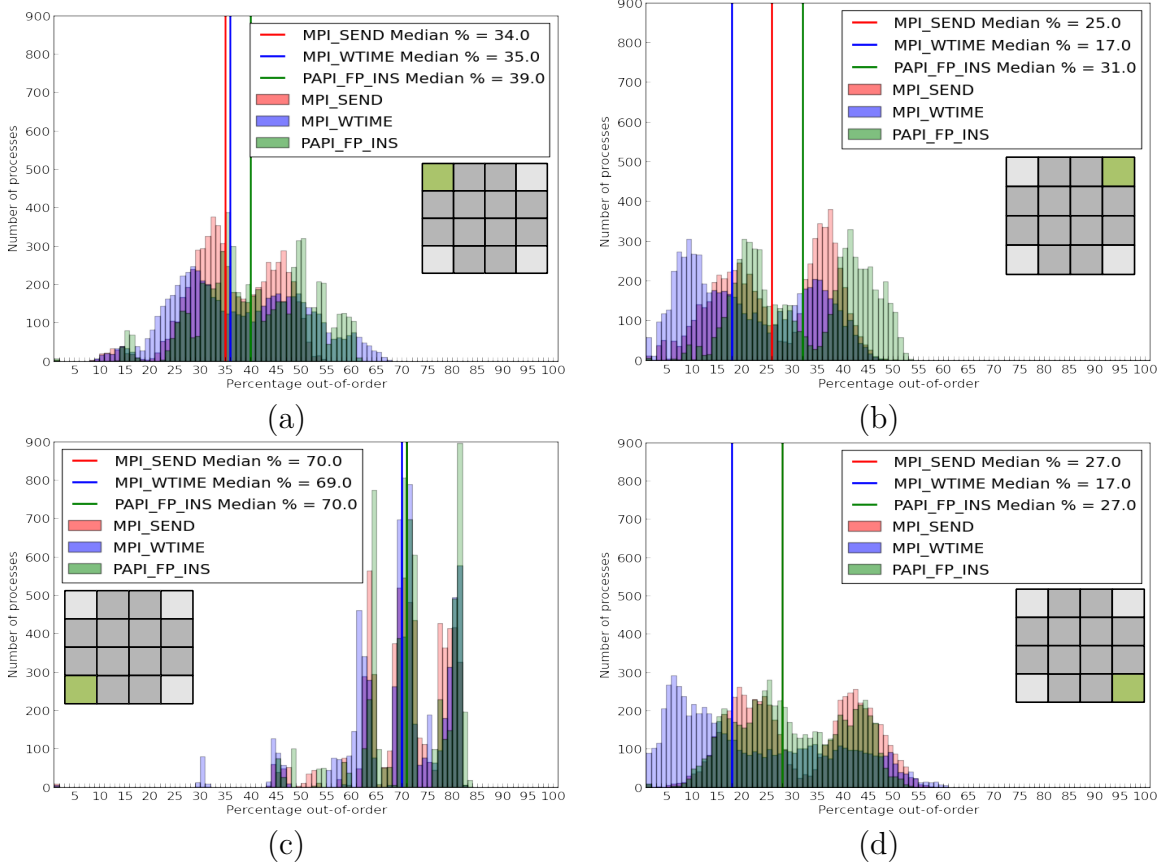


**Figure 3.10:** Distributions of out-of-order message percentages and median out-of-order percentage for each ticking policy over all executions on **four nodes** of Vulcan. The test cases are: 1K particles per process, buffer size 5 (a); 1K particles per process, buffer size 5K (b); 1M particles per process, buffer size 5 (c); and 1M particles per process, buffer size 5K (d).

### 3.10 Lessons Learned

The work in this chapter was motivated from the question whether a ticking policies that resembles the non-replayable wall-clock ticking policy such as our FLOPs-based ticking policies can outperform the baseline ticking policy built into ReMPI.

By comparing the performances of our FLOPs-based ticking against the baseline ticking policy built into ReMPI and a non-replayable wall-time-based ticking policy in four distinct scenarios, we have begun to develop insight into the interaction between



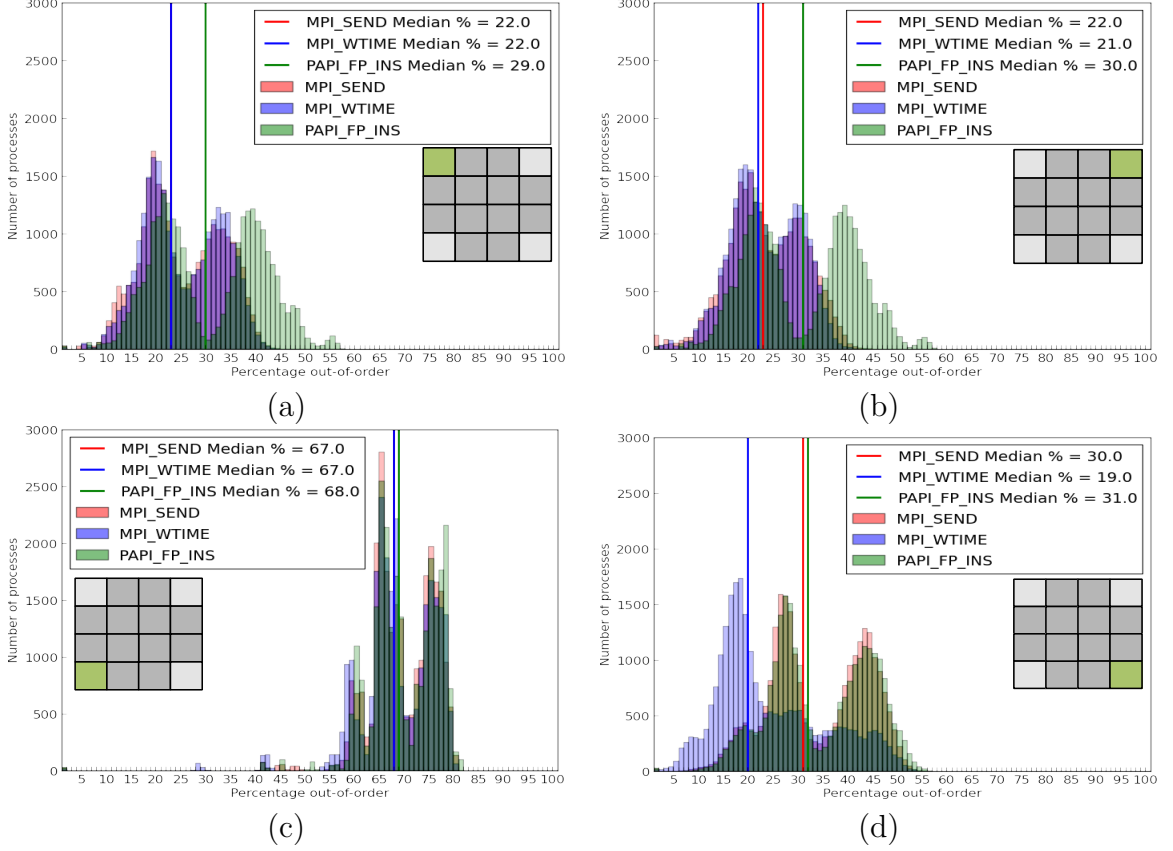


**Figure 3.11:** Distributions of out-of-order message percentages and median out-of-order percentage for each ticking policy over all executions on **16 nodes** of Vulcan. The test cases are: 1K particles per process, buffer size 5 (a); 1K particles per process, buffer size 5K (b); 1M particles per process, buffer size 5 (c); and 1M particles per process, buffer size 5K (d).

application behaviors and the effectiveness of different ticking policies. Although we were not able to observe improvement in median out-of-order percentage for the baseline ticking policy built into our FLOPs-based ticking relative to the baseline ticking policy built into ReMPI, we posit that our ticking policy may still form the basis of a future ticking policy that takes additional application-level information into account to reduce the out-of-order message rate. Additionally, we posit that applications exhibiting greater imbalance between processes' floating-point workloads may benefit more from FLOPs-based ticking policies than MCB does.

One aspect we need to consider is that the MCB application does not have one single communication pattern that is a source of non-determinism, In other words, the tests we showed in this chapter do not identify whether the out-of-order messages are more caused by one of the three patterns. This aspect is further discussed in the next chapter.

## Chapter 4

### CONCLUSION AND FUTURE WORK

#### 4.1 Introduction

In this chapter, we outline the directions of our future research on non-determinism and its impact on reproducibility of HPC applications. So far, we have discussed the numerical challenge of reproducibility in HPC separately from the debugging challenge; work in progress seeks to establish connections between the two problems and their solutions. To this end, in future work we will study connections between run-to-run numerical variability in large scale applications (as explored in Chapter 2) and non-deterministic communication patterns identified with record-and-replay tools (as explored in Chapter 3). The study and generalization of non-deterministic communication patterns not only addresses un-answered questions that were raised in the previous chapter, but also provides a platform for identifying code motifs in applications that lack in numerical reproducibility. We will build our work on non-deterministic communication patterns on top of preliminary findings from our attempts to attribute out-of-order receives to particular communication patterns in MCB described in the next section. The non-determinism in communication patterns cannot be addressed without the development of better ticking policies that mitigate the number of out-of-order events in HPC applications. Therefore we will look at strategies to improve the results presented in Chapter 3.

#### 4.2 Out-of-Order Events and Communication Patterns

In Chapter 3 we investigate the overall rate of out-of-order messages originating from any of three communication patterns in MCB (i.e., the neighbor-to-neighbor particle exchange, the non-blocking gather, and the non-blocking scatter in Figure 3.7).

In this section, we refine our perspective by presenting data on the messages exchanged between particular pairs of processes which, combined with knowledge of which processes receive from which others during each communication pattern, provides insight into which communication patterns are responsible for the majority of out-of-order message receives.

To capture the specific senders of out-of-order messages to each receiving process for each communication pattern, we instrumented the ReMPI code to write to a log file for each received message. Note that the log file is separate from the actual record file generated for ReMPI use during replay. We repeated the tests described in Figure 3.8. For each of the four cells in Figure 3.8, we built a first heatmap with total number of messages and a second heatmap with the total out-of-order messages. Specifically, in the first heatmap, for each receiving process on the row of the heatmap, we collected the total number of messages this process receives from each sending process on the columns of the heatmap; the second heatmap is built in the same way but with the number of out-of-order messages. The intensity of a cell’s coloring in the two heatmaps indicates the number of messages. Cells colored grey indicate that no messages are communicated between the process on the cell’s row (receiving process) and the process on the cell’s column (sending process).

Figure 4.2 shows the total number of messages received by each receiving process from each process that sent to it. This data is collected from a 1-node, 16-process run of MCB which was recorded using ReMPI with MPI\_SEND-ticking (the best of the two replayable record-and replay techniques in Chapter 3. Figure 4.2.(a) refer to high communication intensity with low floating-point workload (i.e., 1K particles per process with a buffer size of 5); Figure 4.2.(b) refers to low communication intensity with low floating point workload (i.e., 1K particles per process with a buffer size of 5K); Figure 4.2.(c) refers to low communication intensity with high floating-point workload (i.e., 1M particles per process, with a buffer size of 5); and Figure 4.2.(d) refers to high communication intensity with low floating-point workload (i.e., 1M particles per process, with a buffer size of 5K).

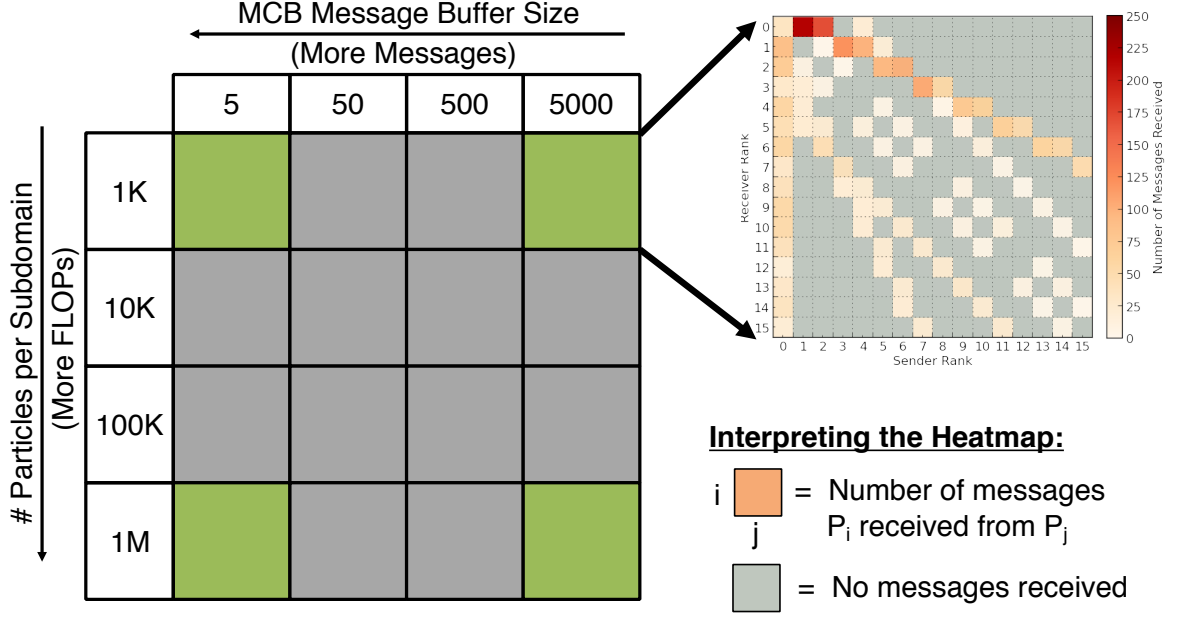
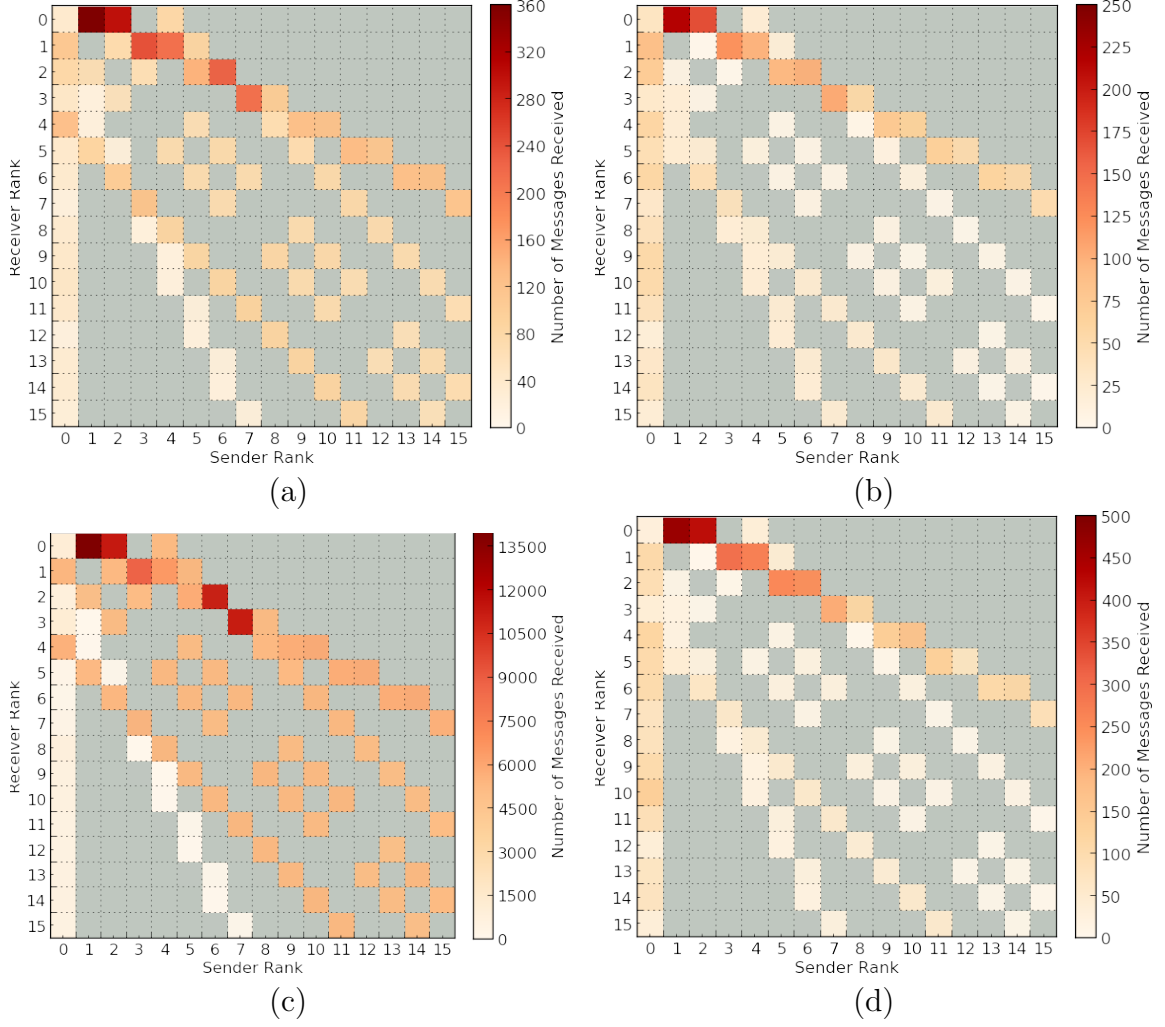


**Figure 4.1:** Interpreting a heatmap of message receives. The receiving processes are listed per row; the sending processes are listed per column.

Figure 4.3 shows heatmaps counting only the out-of-order receives. This data is a subset of that shown in Figure 4.2 and refers to the same four communication intensity and floating-point workload scenarios studied above.

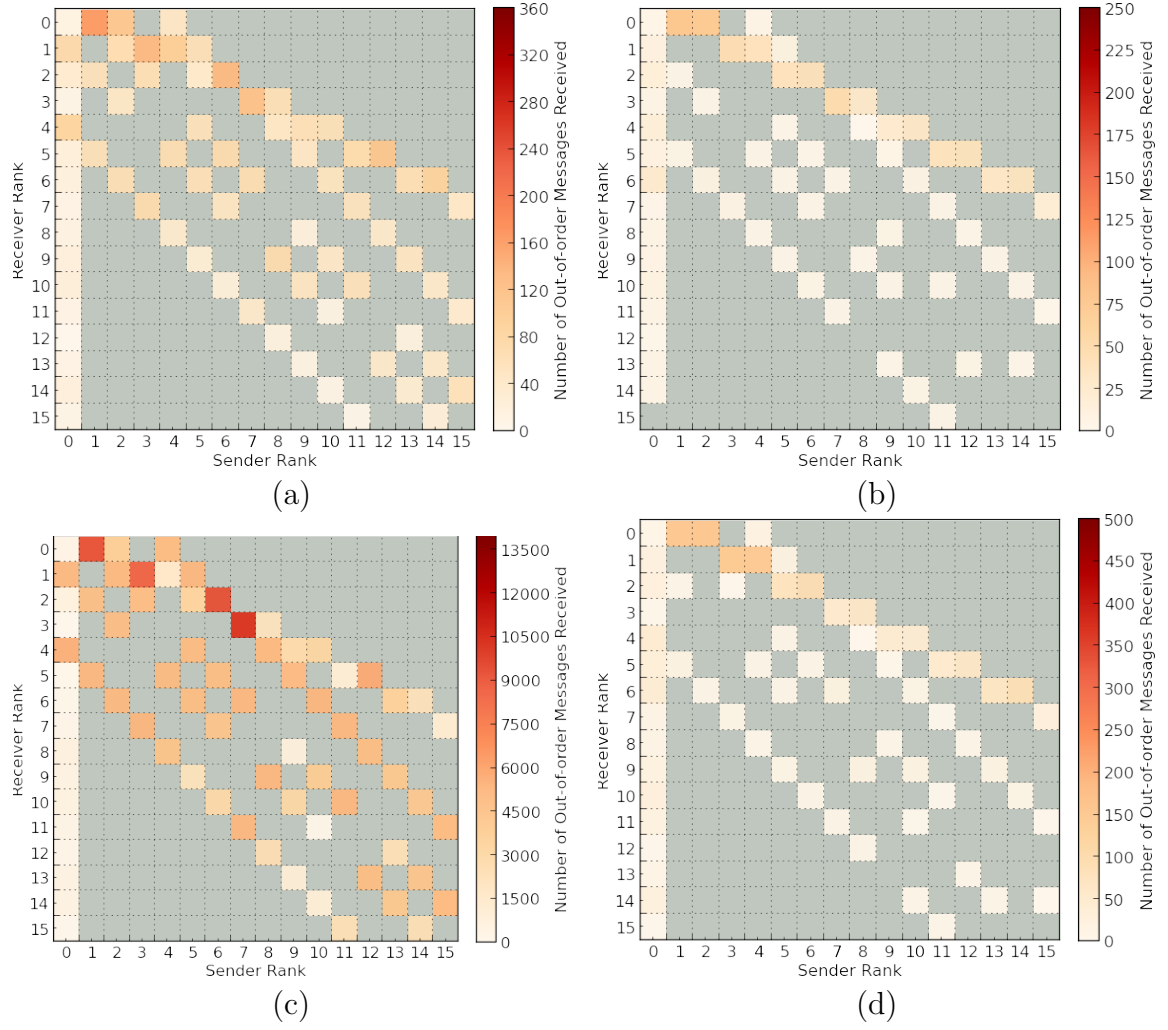
The heatmaps with the total number of communicated message in Figure 4.2 outline how some processes only receive from some other processes during certain communication patterns. For example, process  $P_0$  does not receive messages from process  $P_2$  during the neighbor-to-neighbor particle exchange, but does receive messages from process  $P_2$  during the nonblocking gather. The four heatmaps in the figure confirm the three communication patterns that we had previously extracted with the manual inspection of the MCB code in Figure 3.7.

The inspection of the heatmaps of out-of-order messages outline which one, if any, of the three communication patterns impacts the non-determinism the most. In



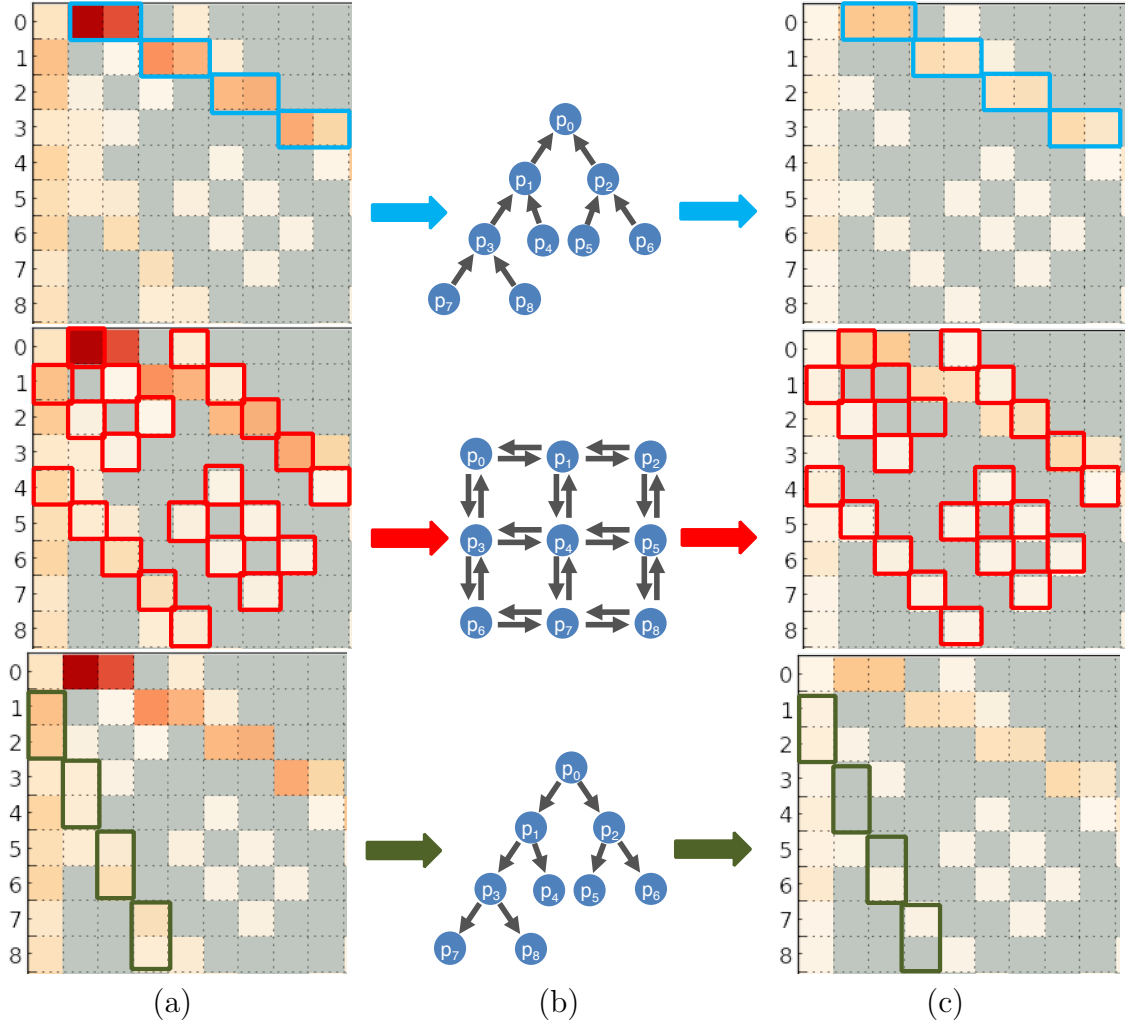
**Figure 4.2:** Total number of messages received by each receiving process  $i$  per sender process  $j$  for a testcase of 1K particles per process, buffer size 5 (a); 1K particles per process, buffer size 5K (b); 1M particles per process, buffer size 5 (c); and 1M particles per process, buffer size 5K (d).

Figure 4.3 we observe that the nonblocking gather pattern is responsible for a disproportionate amount of the out-of-order messages received. In Figure 4.4, we highlight cells of the heatmaps to indicate attribution of out-of-order receives to particular communication patterns. Once again we observe that cells indicating the greatest number of out-of-order receives correspond to messages sent during the non-blocking gather communication pattern, whereas the non-blocking scatter pattern exhibits the least.



**Figure 4.3:** Total number of out-of-order messages received by each receiving process  $i$  per sender process  $j$  for a test case of 1K particles per process, buffer size 5 (a); 1K particles per process, buffer size 5K (b); 1M particles per process, buffer size 5 (c); and 1M particles per process, buffer size 5K (d).

These results are a first insight in the impact of single communication patterns on non-determinism.



**Figure 4.4:** Linking out-of-order receives to one of the three MCB communication patterns presented in Figure 3.7. Because of space constraints only a quarter of each heatmap is shown. Each row shows heatmaps with receiving processes highlighted that participate in a given communication pattern. Column (a) shows heatmaps of total number of receives; column (b) shows the communication pattern; and column (c) shows heatmaps of the number of out-of-order receives.



### 4.3 Adaptive Ticking Policies

Our observation that particular out-of-order receives can be attributed to particular communication patterns suggests a general technique for improving a ticking policy. We propose to develop an *adaptive ticking policy* that is based on application-level events such as floating-point instructions, but also takes into account processes' placement in the communication topology and the phase of communication the application is currently engaged. Our future work in on adaptive ticking policies will proceed along two branches.

We will first expand our investigation of communication patterns that are found in non-deterministic HPC applications, and enrich our understanding of how these communication patterns interact, specifically, with ticking policies, and more generally, with record and replay tools. We will progress this line of research by identifying non-deterministic communication patterns in real applications, modeling their critical characteristics, and developing microbenchmarks based on these patterns so that their responses to ticking policies and record-and-replay tools can be studied in isolation. By doing so, we will systematize adaptation of tools to applications.

Second, we will investigate the feasibility of enhancing ticking policies such as our FLOPs-ticking with high-level information about application behavior, such as what kind of communication pattern the application is currently engaged in. Since we have shown that a ticking policy that works well in one scenario (e.g., low communication intensity and low floating-point workload) may not offer the same benefits in another scenario, it behooves us to investigate the feasibility of ticking policies that can adapt to application characteristics on the fly.

### 4.4 Investigating Numerical Irreproducibility via Record-and-replay

In addition to gleaning insight into how patterns of non-deterministic communication impact the cost of applying record-and-replay techniques such as CDC, our efforts to develop a taxonomy of non-deterministic communication patterns will provide insight into how numerical accuracy is impacted by non-deterministic communication.

Specifically, the ordering of receives in message-passing applications impacts numerical reproducibility of those applications when variability in message arrivals re-orders floating-point operands. We will explore the use of record-and-replay tools for capturing executions exhibiting highly accurate results, as well as those exhibiting highly inaccurate results, in order to ascertain the internal properties of those executions that induced, respectively, accuracy or inaccuracy.

#### 4.5 Summary

In this thesis, we tackled the dual challenges of loss of numerical reproducibility and loss of debuggability that non-determinism in HPC applications presents. In response to the numerical challenge we presented a strong case for selection of summation algorithms based on characteristics of the floating-point operands an application is likely deal with, and showed a quantitative comparison of compensated summation algorithms' responses to the dynamic range and conditioning of their inputs.

In response to the debugging challenge, we investigated a fine-grained logical clock ticking policy based on floating-point operations for use in the Clock-Delta Compression record-and-replay technique. Although our ticking policy did not provide immediate improvements over the baseline ticking policy of CDC, we have demonstrated the feasibility of implementing ticking policies based on application level events, and we present preliminary findings support further investigation into ticking policies that mold themselves to applications' communication patterns. Finally, we propose to merge approaches from both the numerical and debugging perspectives on non-determinism in HPC applications in order to develop general methodologies for addressing the reproducibility challenge.

## BIBLIOGRAPHY

- [1] MCB: Monte Carlo Benchmark.
- [2] Top Ten Exascale Research Challenges. Technical report, Department of Energy (DOE), February 2014.
- [3] D.H. Bailey. High-precision Floating-point Arithmetic in Scientific Computation. In *Computing in Science and Engineering*, 2005.
- [4] P. Balaji and D. Kimpe. On the Reproducibility of MPI Reduction Operations. In *Proc of the IEEE International Conference on High Performance Computing and Communications (HPCC)*, November 2013.
- [5] F. Cappello, A. Guermouche, and M. Snir. On communication determinism in parallel HPC applications. In *Computer Communications and Networks (ICCCN), 2010 Proceedings of 19th International Conference on*, pages 1–8, Aug 2010.
- [6] A. Castaldo. Error Analysis of Various Forms of Floating Point Dot Products. Master’s thesis, University of Texas at San Antonio, August 2007.
- [7] W.-F. Chiang, G. Gopalakrishnan, Z. Rakamaric, Dong H. Ahn, and G.L. Lee. Determinism and Reproducibility in Large-scale HPC Systems. In *Proc. of the 4th Workshop on Determinism and Correctness in Parallel Programming (WoDet)*, 2013.
- [8] C. Cl  men  on, J. Fritscher, M. J. Meehan, and R. R  hl. An implementation of race detection and deterministic replay with MPI. In *Proceedings of the First International Euro-Par Conference on Parallel Processing*, Euro-Par ’95, pages 155–166, London, UK, UK, 1995. Springer-Verlag.
- [9] M. A. Cleveland, T. A. Brunner, N. A. Gentile, and J. A. Keasler. Obtaining identical results with double precision global accuracy on different numbers of processors in parallel particle Monte Carlo simulations. *J. Comput. Phys.*, 251:223–236, October 2013.
- [10] J. Demmel and Y. Hida. Accurate and Efficient Floating Point Summation. *SIAM J. Sci. Comp.*, 25(4):1214–1248, 2003.
- [11] J. Demmel and H.D. Nguyen. Parallel Reproducible Summation. *IEEE Transactions on Computers*, 64(7):2060–2070, 2015.

- [12] J. Dongarra. The MPI Profiling Interface, 1995.
- [13] C. J. Fidge. Timestamps in message-passing systems that preserve the partial ordering. *Proceedings of the 11th Australian Computer Science Conference*, 10(1):5666, 1988.
- [14] Y. He and C.H.Q. Ding. Using Accurate Arithmetics to Improve Numerical Reproducibility and Stability in Parallel Applications. In *Proc. of the 14th International Conference on Supercomputing (ICS)*, pages 225–234, 2000.
- [15] N. J. Higham. The Accuracy of Floating Point Summation. *SIAM J. Sci. Comput.*, 14(4):783–799, July 1993.
- [16] F. Jézéquel, P. Langlois, and N. Revol. First Steps Towards more Numerical Reproducibility. *ESAIM: Proceedings*, 45:229–238, September 2014.
- [17] W. Kahan. Pracniques: Further Remarks on Reducing Truncation Errors. *Communications of the ACM*, 8(1):40–, January 1965.
- [18] D. Kranzlmüller and J. Volkert. NOPE: A nondeterministic program evaluator. In *Proceedings of the 4th International ACPC Conference Including Special Tracks on Parallel Numerics and Parallel Computing in Image Processing, Video Processing, and Multimedia: Parallel Computation*, ParNum ’99, pages 490–499, London, UK, UK, 1999. Springer-Verlag.
- [19] L. Lamport. Time, clocks, and the ordering of events in a distributed system. *Commun. ACM*, 21(7):558–565, July 1978.
- [20] P. Langlois, M. Martel, and L. Thévenoux. Accuracy Versus Time: A Case Study with Summation Algorithms. In *Proc. of the 4th International Workshop on Parallel and Symbolic Computation (PASCO)*, pages 121–130, 2010.
- [21] R. H. B. Netzer and B. P. Miller. Optimal tracing and replay for debugging message-passing parallel programs. In *Proceedings of the 1992 ACM/IEEE Conference on Supercomputing*, Supercomputing ’92, pages 502–511, Los Alamitos, CA, USA, 1992. IEEE Computer Society Press.
- [22] H.D. Nguyen and J. Demmel. Reproblas: Reproducible blas. <http://bebop.cs.berkeley.edu/reproblas/>.
- [23] R. Robey, J. Robey, and R. Aulwes. In search of numerical consistency in parallel programming. *Parallel Computing*, 37(4):217–229, April 2011.
- [24] C. Rubio-González, C. Nguyen, H.D. Nguyen, J. Demmel, W. Kahan, K. Sen, D.H. Bailey, C. Iancu, and D. Hough. Precimonious: Tuning Assistant for Floating-point Precision. In *Proc. of the International Conference on High Performance Computing, Networking, Storage and Analysis (SC)*, 2013.

- [25] K. Sato, D. H. Ahn, I. Laguna, G. L. Lee, and M. Schulz. Clock delta compression for scalable order-replay of non-deterministic parallel applications. In *Proceedings of the International Conference for High Performance Computing, Networking, Storage and Analysis*, SC '15, pages 62:1–62:12, New York, NY, USA, 2015. ACM.
- [26] K. Sato, D. H. Ahn, I. Laguna, G. L. Lee, M. Schulz, and C. M. Chambreau. Noise injection techniques to expose subtle and unintended message races. In *Proceedings of the 20th ACM SIGPLAN Symposium on Principles and Practice of Parallel Programming*, PPOPP '17.
- [27] M. Schulz and B.R. de Supinski. PNMPI tools: a whole lot greater than the sum of their parts. In *Supercomputing, 2007. SC '07. Proceedings of the 2007 ACM/IEEE Conference on*, pages 1–10, Nov 2007.
- [28] M. Taufer, O. Padron, P. Saponaro, and S. Patel. Improving Numerical Reproducibility and Stability in Large-scale Numerical Simulations on GPUs. In *Proc. of the IEEE International Symposium on Parallel Distributed Processing (IPDPS)*, pages 1–9, April 2010.